

Binary Lenses in OGLE-III EWS Database. Seasons 2006–2008

M. Jaroszyński¹, J. Skowron^{2,1}, A. Udalski¹, M. Kubiak¹,
M. Szymański¹, G. Pietrzyński¹, I. Soszyński¹, Ł. Wyrzykowski³,
K. Ulaczyk¹, and R. Poleski¹

¹Warsaw University Observatory, Al. Ujazdowskie 4, 00-478 Warszawa, Poland
e-mail:(mj,jskowron,udalski,mk,msz,pietrzyn,soszynsk,kulaczyk,rpoleski)
@astrouw.edu.pl

²Department of Astronomy, The Ohio State University, 140 W. 18th Ave.,
Columbus, OH 43210, USA

³Institute of Astronomy, Cambridge University, Madingley Road,
Cambridge CB3 0HA, UK
e-mail:wyrzykow@ast.cam.ac.uk

ABSTRACT

We present 27 binary lens candidates from OGLE-III Early Warning System database for the seasons 2006–2008. The candidates have been selected by visual light curves inspection. Our sample of binary lens events consists now of 78 stellar systems and 7 extrasolar planets of OGLE-III published elsewhere. Examining the distribution of stellar binaries we find that the number of systems per logarithmic mass ratio interval increases with mass ratio q , in contradiction with our previous findings. Stellar binaries belong to the region $0.03 < q < 1$ and there is a gap between them and a separate population of planets.

Gravitational lensing – Galaxy: center – binaries: general

1 Introduction

In this paper we present the results of the search for binary lens events among microlensing phenomena discovered by the Early Warning System (EWS – Udalski *et al.* 1994, Udalski 2003) of the third phase of the Optical Gravitational Lensing Experiment (OGLE-III) in the seasons 2006–2008. Since OGLE-III Phase ended early in 2009, and we do not find any binary lens candidates with complete light curves discovered by EWS in this season, this paper finishes our presentation of binary lens candidates among OGLE-III events. Our study is the continuation of work on binary lenses in OGLE-II (Jaroszyński 2002, hereafter Paper I) and OGLE-III databases (Jaroszyński *et al.* 2004, hereafter Paper II Jaroszyński *et al.* 2006, hereafter Paper III, and Skowron *et al.* 2007, hereafter Paper IV). The results of the similar search for binary lens events in MACHO data have been presented by Alcock *et al.* (2000).

The motivation of the study remains the same – we are going to obtain a uniform sample of binary lens events, selected and modeled with the same methods for all seasons. The sample may be used to study the population of binary systems in the Galaxy. The method of observation of the binaries (gravitational lensing) allows to study their mass ratios distribution, since they are directly given by the models. The binary separations are more difficult, because only their projection into the sky expressed in Einstein radius units enters the models. In small number of cases the estimation of the masses and distances to the lenses may be possible.

Cases of extremely low binary mass ratios ($q \leq 0.01$) are usually considered as planetary lensing. Models of six microlensing planetary events from the OGLE-III database have been published (OGLE-2003-BLG-235 / MOA-2003-BLG-53 Bond *et al.*, 2004; OGLE-2005-BLG-071 Udalski *et al.* 2005; OGLE-2005-BLG-169 Gould *et al.* 2006; OGLE-2005-BLG-390 Beaulieu *et al.* 2006; OGLE-2006-BLG-109 Gaudi *et al.* 2008; OGLE-2007-BLG-368 Sumi *et al.* 2010). Since the event OGLE-2006-BLG-109 is modeled as caused by a star with two planets, there are seven planets with known mass ratios.

The adequate modeling of a planetary event requires frequent round the clock observations of the source, which is achieved by cooperation of observers at different longitudes on Earth. In cases of less extreme lenses, the observations of single telescope may be sufficient to obtain well constrained models of the systems. The present analysis is based on the OGLE-III data alone.

Our approach follows that of Papers I, II, III and IV, where the references to earlier work on the subject are given. Some basic ideas for binary lens analysis can be found in the review article by Paczyński (1996). Paper I presents the analysis of 18 binary lens events found in OGLE-II data with 10 safe caustic crossing cases. There are 15 binary lens events reported in Paper II, 19 in Paper III, and 9 in Paper IV. The event OGLE-2003-BLG-235 included in Paper II is a planetary lens, and the binary lens interpretation of the event OGLE-2005-BLG-226 of Paper IV is less convincing than for other cases, so these two events are not included in our sample of stellar binary lenses.

In Section 2 we describe the selection of binary lens candidates. In Section 3 we describe the improvements of the fitting procedure as compared to our previous articles on the subject. The results are described in Section 4, and the discussion follows in Section 5. The extensive graphical material is shown in Appendix.

2 Choice of Candidates

The OGLE-III data is routinely reduced with difference photometry (DIA, Alard and Lupton 1998, Alard 2000) which gives high quality light curves of variable objects. The EWS system of OGLE-III (Udalski 2003) automatically picks up candidate objects with microlensing-like variability.

There are 581 microlensing event candidates selected by EWS in the season of 2006, 610 in 2007, 654 in 2008, and 156 in 2009. We visually inspect all candidate light curves looking for features characteristic for binary lenses (multiple peaks, U-shapes, asymmetry). Light curves showing excessive noise are omitted. We select 31 candidate binary events from the data for further study. For these candidate events we apply our standard procedure of finding binary lens models (compare Papers I–IV and Section 3).

3 Fitting Binary Lens Models

The models of the two point mass lens were investigated by many authors (Schneider and Weiss 1986, Mao and Paczyński 1991, Mao and DiStefano 1995, DiStefano and Mao 1996, Dominik 1998, to mention only a few). The effective methods applicable for extended sources were described by Mao and Loeb (2001). We follow their approach and use image finding algorithms based on the Newton method. Our approach has been described in Papers I–IV. We have technically improved the search for models in cases of caustic crossing events, using different, more *natural* parametrization of the models in the calculations, following Cassan (2008) and Skowron (2009). In reporting

our results we use the notation of Papers I–IV; below we describe our convention for completeness.

We fit binary lens models using the χ^2 minimization method for the light curves. It is convenient to model the flux at the time t_i as:

$$F_i = F(t_i) = A(\mathbf{p}; t_i) \times F_s + F_b \equiv (A(\mathbf{p}; t_i) - 1) \times F_s + F_0 \quad (1)$$

where $A(\mathbf{p}; t_i)$ is the binary lens amplification at instant t_i calculated with the model defined by a set of parameters \mathbf{p} , F_s is the flux of the source being lensed, F_b the blended flux (from the source close neighbors and possibly the lens), and the combination $F_b + F_s = F_0$ is the total flux, measured long before or long after the event. The baseline flux (F_0) can be reasonably well estimated with observations performed in seasons when the source was not showing variability (see below). The binary lens parameters (\mathbf{p}) are: the mass ratio q , the binary separation d , the source trajectory direction β , the impact parameter b relative to the lens center of mass, the time of the closest center of mass approach t_0 , the Einstein time t_E , the size of the source r_s . The separation (d), impact parameter (b) and source radius (r_s) are all expressed in Einstein units.

In fitting the models we use rescaled errors (compare Papers I–IV). More detailed analysis (*e.g.*, Wyrzykowski 2005, Skowron 2009, Skowron *et al.* 2009) shows that the OGLE photometric errors are overestimated for very faint sources and underestimated for bright ones. Error scaling used here, based on the scatter of the observed flux in seasons when the source is supposedly invariable, is the simplest approach. It gives the estimate of the combined effect of the observational errors and possibly undetectable, low amplitude internal source variability. We require that constant flux source model fits well the other seasons data after introducing error scaling factor s :

$$\chi_{\text{other}}^2 = \sum_{i=1}^{N'} \frac{(F_i - F_0)^2}{(s\sigma_i)^2} = N' - 1 \quad (2)$$

where F_0 is the optimized value. The summation is over N' data points, which do not belong to the event's season. Our analysis of the models, their fit quality etc is based on the χ_1^2 calculated with the rescaled errors:

$$\chi_1^2 \equiv \frac{\chi^2}{s^2} \quad (3)$$

which is displayed in the tables and plots. For events with multiple models (representing different local minima of χ^2), we assess the relevance of each model with the relative weight $w \sim \exp(-\chi_1^2/2)$.

Only the events with characteristics of caustic crossing (apparent discontinuities in observed light curves, U-shapes) can be treated as safe binary lens cases. The double peak events may result from cusp approaches, but may also be produced by double sources (*e.g.*, Gaudi and Han 2004). In such cases we check also the double source fit of the event postulating:

$$F(t) = A_s(u_1(t)) \times F_{s1} + A_s(u_2(t)) \times F_{s2} + F_b \quad (4)$$

where F_{s1} , F_{s2} are the fluxes of the source components, F_b is the blended flux, u_i are the distances between the source components and the lens expressed in Einstein units, and $A_s(u)$ is the single lens amplification (Paczynski, 1986).

4 Results

Our fitting procedures applied to 31 candidate events selected give the results summarized in Table 1. Models of the two events (2006-BLG-038 and 2006-BLG-460) have

already been published by Skowron *et al.* (2009). Our calculations give very similar sets of parameters for these two events. Some events have two or three substantially different models of similar fit quality and in such cases we present all of them. We do not include models of planetary events published elsewhere.

In the second column of the table we assess the character of the events. In 27 cases (of 31 investigated) the events are safe binary lens phenomena in our opinion (designated “b” in Table 1). There are two cases classified as double source events (“d” in Table 1) and two events with a low quality, unsatisfactory fit (“u” in Table 1). The source paths and model light curves are shown in the first part of Appendix.

Some events have double peaks, but do not show any sharp changes in their light curves. In such cases we try double source models. If double source models are acceptable, we skip binary lens modeling. In some cases we present models of both kinds. Results of double source modeling are presented in Table 2. The model light curves are shown in Appendix.

While our double source models usually give formally good fits of the light curves, not all of them are realistic. There are cases degenerated, where one or both source components are very weak, but visible due to very small impact parameters and very large amplifications. The Einstein times for such models are also unrealistically long. Since double sources modeling are not our primary goal, we do not further pursue this topic.

Our sample of binary lenses consists now of 78 events of Papers I–IV, and the present work, some of them with multiple models, plus 6 published OGLE-III planetary events, which we also include. Using the sample we may study the distributions of various binary lens parameters. In Fig.1 we show the distribution of the mass ratio. In the left panel the observed distributions of planetary and binary events are shown on the same plot. The two kinds of events are not overlapping: the binary stars with mass ratio $q < 0.03$ are not present in our sample.

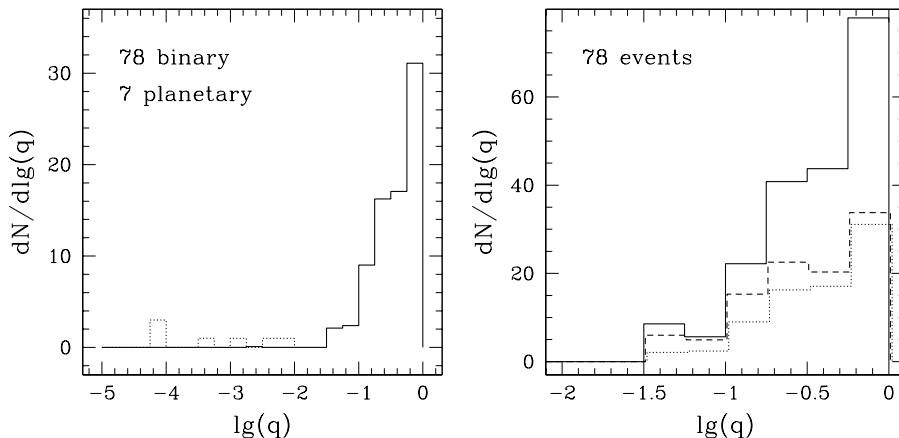


Fig. 1. The histograms for the mass ratios. In the *left panel* we show the distribution of binary lens ratios (solid line) found in Papers I–IV and in this work with superimposed data for OGLE-III planetary events (dotted) published elsewhere. In the *right panel* we compare the raw distribution for binaries (dotted) with the distribution corrected for selection effects with the help of method I (dashed) and II (solid). Corrected histograms are multiplied by artificial factors to avoid crossings of the plots.

The observed distribution of the mass ratio (or any other binary lens parameter) depends on its intrinsic distribution and on the observational selection. The contribution of the binary lenses to the rate of microlensing events depends on many parameters. Modifying formulae applicable to single lens (Griest 1991, Kiraga and Paczyński 1994, Wood and Mao 2005) and neglecting the part describing the source, one has for

a binary lens:

$$\Delta\Gamma \propto n(m, q, d, R_{\text{OL}}) S(q, d) r_E f(v) v \quad (5)$$

where n is the number density of binary systems of total mass m , mass ratio q , separation d , and the distance from the observer R_{OL} ; r_E is the Einstein radius, v is the relative source–lens velocity component perpendicular to the line of sight, and $f(v)$ is its distribution function. $S(q, d)$ is the angle averaged width of the caustic, expressed in Einstein units, which gives the relative probability of a caustic crossing event caused by a binary of given caustic size and topology. The trajectory of a source has to pass sufficiently close to a caustic to cause a non crossing event distinguishable from point lens microlensing, so the relative probability is roughly given by $S(q, d)$ also in this case. In the case of planetary events, where the duration of the caustic region crossing plays a role in detection efficiency, the length of the source trajectory inside caustic may also be a factor worth consideration making the rate of the detection proportional to the caustic surface area in the simplest approach, but according to Sumi *et al.*, (2010) the dependence on the event duration is much weaker. We neglect the possible dependence of the detection efficiency on the duration of the caustic region crossing / approach in the case of stellar binary lenses.

The full analysis of the *a priori* probability of detecting a binary event, based on stellar mass and velocity distributions goes beyond the scope of this paper. We limit our considerations to the dependence of detection probability on the mass ratio and the binary separation. For everything else equal, the observed and intrinsic distributions of these parameters are related by:

$$N_{\text{obs}}(\lg q, \lg d) \propto f_q(\lg q) f_d(\lg d) S(q, d) \quad (6)$$

where N_{obs} gives the number of observed events in equal logarithmic bins of q and d , and f_q , f_d are the intrinsic distribution functions of these parameters. We have assumed that the intrinsic mass ratio and separation distributions are independent. For any assumed separation distribution one can average both sides of the equation over $\lg d$ obtaining (method I):

$$f_q(\lg q) \propto \frac{\langle N_{\text{obs}}(\lg q, \lg d) \rangle}{\langle f_d(\lg d) S(q, d) \rangle} \quad (7)$$

Another method (II) of finding mass ratio distribution reads:

$$f_q(\lg q) \propto \left\langle \frac{N_{\text{obs}}(\lg q, \lg d)}{f_d(\lg d) S(q, d)} \right\rangle > . \quad (8)$$

In the right panel of Fig. 1 we show the observed and corrected for detection efficiency distribution of the mass ratios for stellar binary lenses. The corrections by methods I and II have been made assuming that the separation distribution is uniform in logarithm ($f_d(\lg d) \propto \text{const}$). All three histograms show that the number of binary systems per logarithmic interval of the mass ratio increases with q .

We also show the observed distributions of the blending factor ($f = F_s/F_0$) and the distribution of the Einstein times (t_E) among the binary lens models belonging to our sample.

5 Discussion

Our sample of OGLE-II–OGLE-III stellar binary lens events contains now 78 cases and we present the distribution of the binary lens mass ratio in Fig. 1. The planetary and

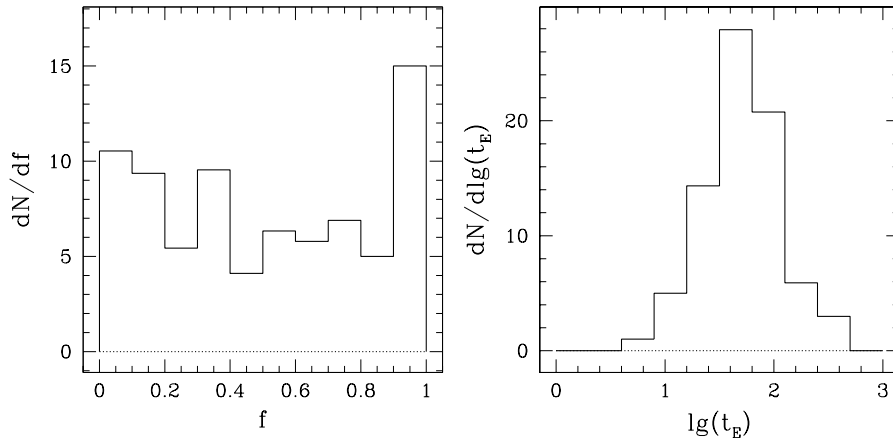


Fig. 2. The histograms for the blending parameter (*left*) and the logarithm of the Einstein time. The plots are not corrected for any selection effects.

stellar binary lenses are clearly separate populations of objects, which do not overlap on our plot. This is not surprising, since the formation scenarios are different for them. It is also impossible to draw any conclusions about the relative rate of planetary and stellar binary events, since the former attract much more attention from astronomers and their discoveries with the microlensing methods result from much larger observational and theoretical effort. Effectively the two samples are based on different databases. The planetary mass function is presented by Sumi *et al.* (2010). We limit our analysis to the stellar binaries.

Our sample of stellar binary lenses covers now the range $0.03 < q < 1$. The observed distribution of number of events per logarithmic mass ratio interval ($dN/d\lg q$) is an increasing function of q . The simple methods of correction for the observational selection effects do not change this conclusion: both raw and corrected histograms show the increase of the number of objects with increasing mass ratio. This conclusion contradicts our earlier view, that the distribution of mass ratios is uniform in logarithm ($dN/d\lg q \propto \text{const}$). According to Trimble (1990) the uniform distribution is appropriate to spectroscopic binaries with orbital periods between 10 and 1000 d, but other kinds of binaries can have different forms of distribution.

Skowron *et al.* (2009) find, that the uniform distribution of mass ratios is consistent with their small sample of binaries causing repeating microlensing events. Simultaneously, under the assumptions of uniform distributions of binaries in $\lg q$ and $\lg d$ they find that all stars should be in binary systems (in contradiction with popular wisdom) to explain the relatively high rate of repeating microlensing events classified as caused by binary lenses. One of the ways to circumvent the contradiction is to change the distribution of mass ratios allowing for relatively higher number of $q \approx 1$ systems, which in turn increases the probability of detection of repeating events caused by binary lenses.

Jaroszyński and Skowron (2008) investigate the role of double sources in explaining the rate of repeating events. Similarly as Skowron *et al.* (2009), and using similar assumptions they find that all sources should be binary systems. Since the luminosity ratio is some positive power of mass ratio (the paper assumes $\propto q^{3.2}$), the sources with small q do not count: the weaker component is practically undetectable. Again, postulating relatively higher number of similar mass systems, one gets relatively higher probability of detection of a repeating event caused by a double source, thus decreasing the required number of binaries among stars.

Our analysis of the mass ratio distribution is still preliminary. We treat all events

modeled as caused by binary lenses as equally important, ignoring the differences in light curve coverage, fit quality, and a priori probability of various physical lens parameters. These topics require further study.

The blending parameter distribution presented in Fig. 2 agrees with the result presented in Paper II. It may also be compared with the distribution obtained by Smith *et al.* (2007) for single microlensing events. In our approach we treat models with blending parameter $f > 1$ as unphysical, since they require negative blended flux. Smith *et al.* (2007) allow larger values of this parameter ($f \leq 2$), interpreting negative fluxes as possible errors of photometric pipeline. In the range $0 \leq f \leq 1$ there is no contradiction between our distribution and their findings.

Acknowledgements. The systematic investigation of binary gravitational lenses in OGLE databases was suggested to us by late Professor Bohdan Paczyński, whose ideas and enthusiasm were an invaluable help in our studies. We thank Shude Mao for the permission of using his binary lens modeling software. This work was supported in part by the Polish Ministry of Science and Higher Education grant N203 008 32/0709 and by Space Exploration Research Fund of The Ohio State University.

REFERENCES

- Alard, C. 2000, *Astron. Astrophys. Suppl. Ser.*, **144**, 363.
 Alard, C., and Lupton, R.H. 1998, *Astrophys. J.*, **503**, 325.
 Alcock, C., *et al.* 2000, *Astrophys. J.*, **541**, 270.
 Beaulieu, J.-P. *et al.* 2006, *Nature*, **439**, 437.
 Bond, I.A. *et al.* 2004, *Astrophys. J.*, **606**, L155.
 Cassan, A. 2008, *Astron. Astrophys.*, **491**, 587.
 DiStefano, R., and Mao, S. 1996, *Astrophys. J.*, **457**, 93.
 Dominik, M. 1998, *Astron. Astrophys.*, **333**, L79.
 Gaudi, B.S., and Han, Ch. 2004, *Astrophys. J.*, **611**, 528.
 Gaudi, B.S., *et al.* 2008, *Science*, **319**, 927.
 Gould, A. *et al.* 2006, *Astrophys. J.*, **644**, L37.
 Griest, K. 1991, *Astrophys. J.*, **366**, 412.
 Jaroszyński, M. 2002, *Acta Astron.*, **52**, 39 (Paper I).
 Jaroszyński, M., and Skowron, J. 2008, *Acta Astron.*, **58**, 345.
 Jaroszyński, M., Udalski, A., Kubiak, M., Szymański, M., Pietrzyński, G., Soszyński, I., Żebruń, K., Szewczyk, O., and Wyrzykowski, Ł. 2004, *Acta Astron.*, **54**, 103 (Paper II).
 Jaroszyński, M., Skowron, J., Udalski, A., Kubiak, M., Szymański, M., Pietrzyński, G., Soszyński, I., Żebruń, K., Szewczyk, O., and Wyrzykowski, Ł. 2006, *Acta Astron.*, **56**, 307 (Paper III).
 Kiraga, M., and Paczyński, B. 1994, *Astrophys. J.*, **430**, L101.
 Mao, S., and DiStefano, R. 1995, *Astrophys. J.*, **440**, 22.
 Mao, S., and Loeb, A. 2001, *Astrophys. J.*, **547**, L97.
 Mao, S., and Paczyński, B. 1991, *Astrophys. J.*, **374**, L37.
 Paczyński, B. 1996, *Ann. Rev. Astron. Astrophys.*, **34**, 419.
 Schneider, P., and Weiss, A. 1986, *Astron. Astrophys.*, **164**, 237.
 Skowron, J. 2009, *PhD Thesis*, , University of Warsaw Astronomical Observatory.
 Skowron, J., Jaroszyński, M., Udalski, A., Kubiak, M., Szymanski, M.K., Pietrzynski, G., Soszynski, I., Szewczyk, O., Wyrzykowski, Ł., and Ulaczyk, K. 2007, *Acta Astron.*, **57**, 281 (Paper IV).
 Skowron, J., Wyrzykowski, Ł., Mao, S., and Jaroszyński, M. 2009, *MNRAS*, **393**, 999.
 Smith, M.C., Woźniak, P., Mao, S., and Sumi, T. 2007, *MNRAS*, **380**, 805.
 Sumi, T., *et al.* 2010, *Astrophys. J.*, **710**, 1641.
 Trimble, V. 1990, *MNRAS*, **242**, 79.
 Udalski, A. 2003, *Acta Astron.*, **53**, 291.
 Udalski, A., *et al.* 2005, *Astrophys. J.*, **628**, L109.
 Udalski, A., Szymański, M., Kaluzny, J., Kubiak, M., Mateo, M., Krzemiński, W., and Paczyński, B. 1994, *Acta Astron.*, **44**, 227.
 Wood, A., and Mao, S. 2005, *MNRAS*, **362**, 945.
 Wyrzykowski, Ł. 2005, *PhD Thesis*, , Warsaw University Astronomical Observatory.

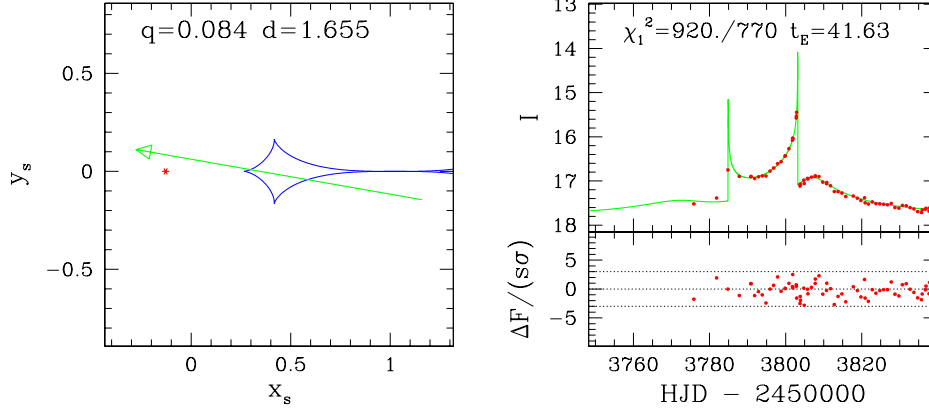
7 Appendix

7.1 Binary lens models

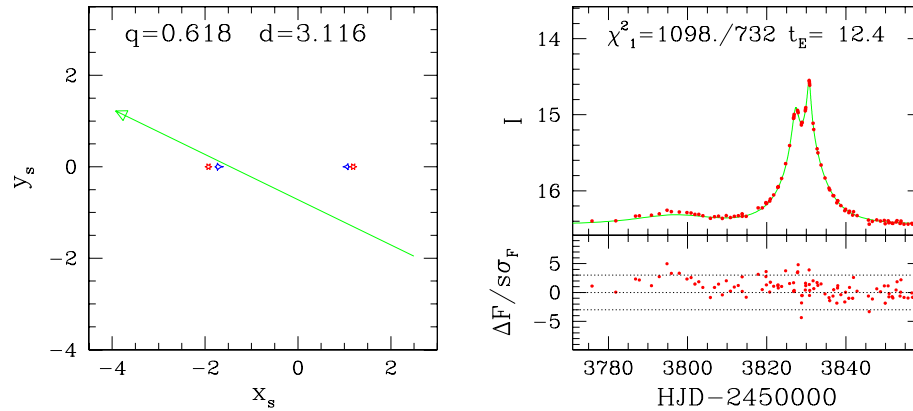
Below we present the plots for the 31 events for which the binary lens modeling has been applied. The events are ordered and named according to their position in the OGLE EWS database. Some of the events, especially cases without apparent caustic crossing, may have alternative double source models. In such cases we show the comparison of the binary lens and double source fits to the data in the next subsection. For events which have multiple, substantially different models of similar quality, we present up to 3 of them.

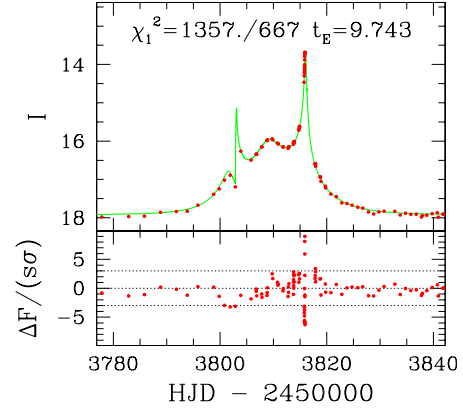
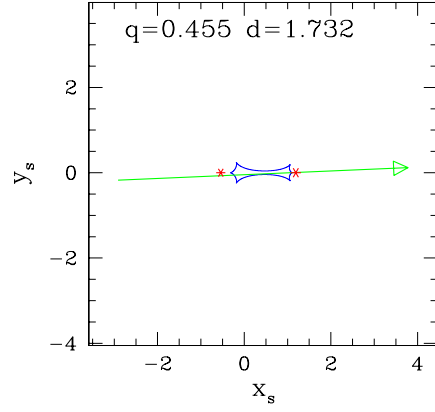
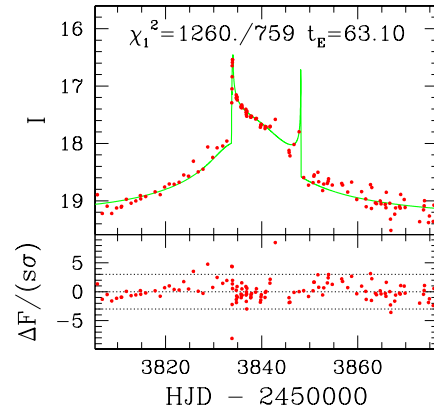
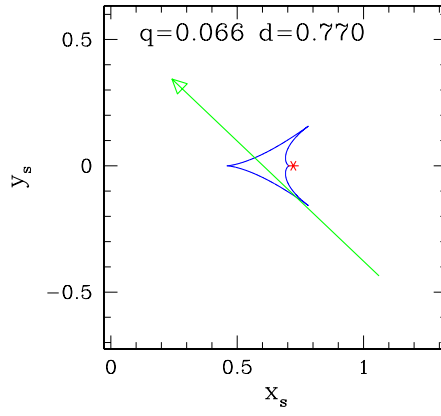
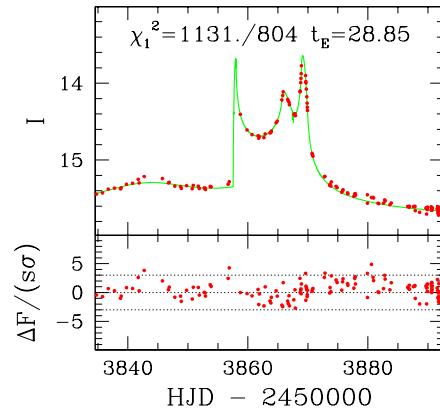
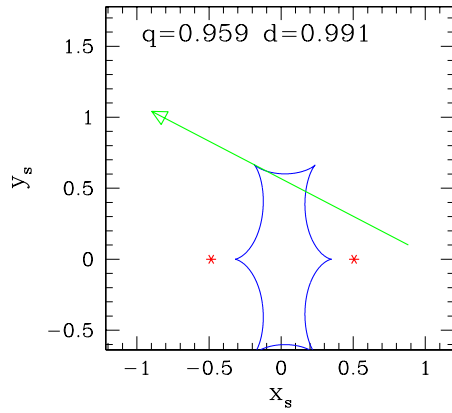
Each case is illustrated with two panels. The most interesting part of the source trajectory, the binary and its caustic structure are shown in the left panel for the case considered. The labels give the q and d values. On the right the part of the best fit light curve is compared with observations. The labels give the rescaled χ_1^2/DOF values and Einstein times resulting from fits. Multiple models of the same event usually have similar model light curves, but have different trajectories, different caustic structure and different values of the Einstein time. Below the light curves we show the differences between the observed and modeled flux in units of rescaled errors. The dotted lines show the rescaled $\pm 3\sigma$ band.

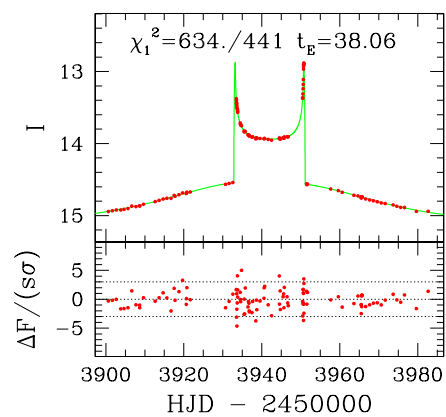
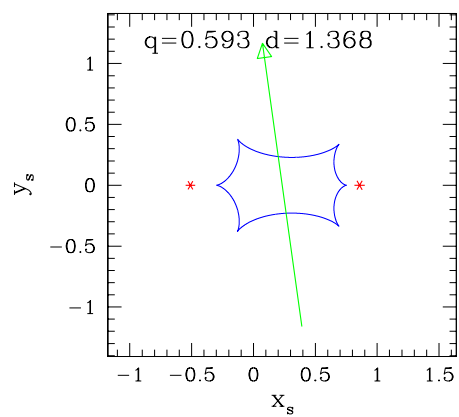
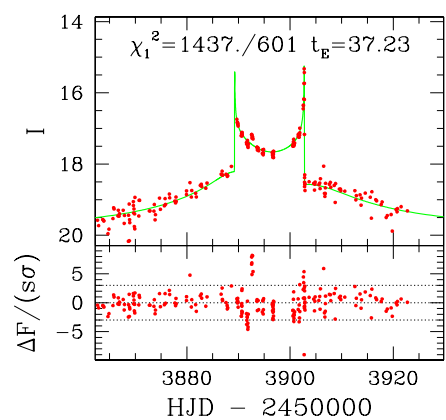
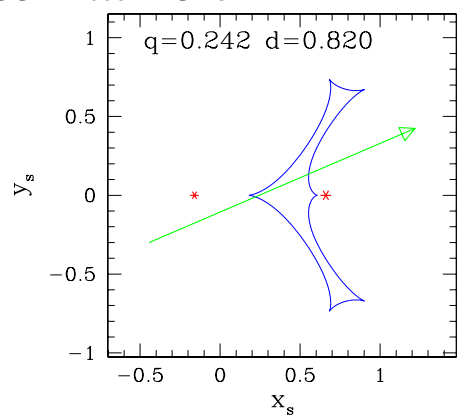
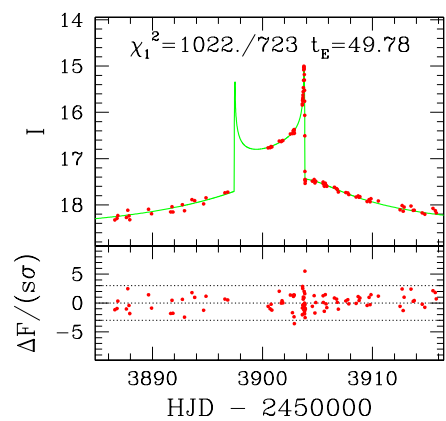
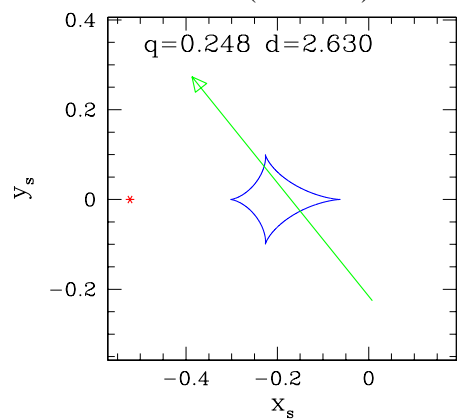
OGLE 2006-BLG-028



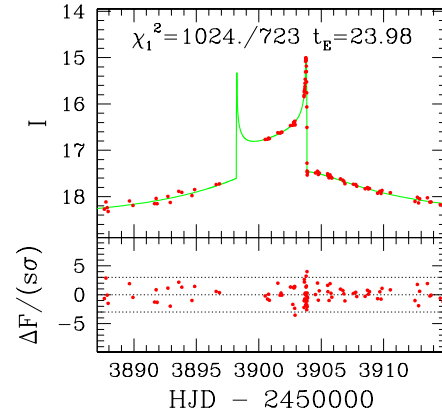
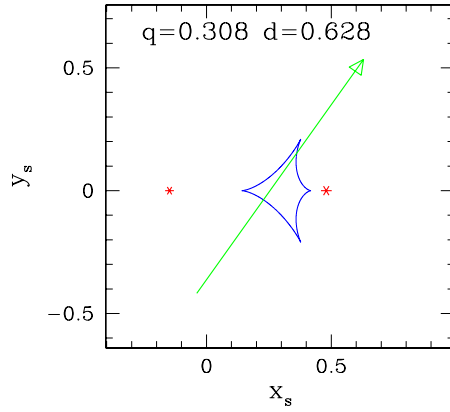
OGLE 2006-BLG-038



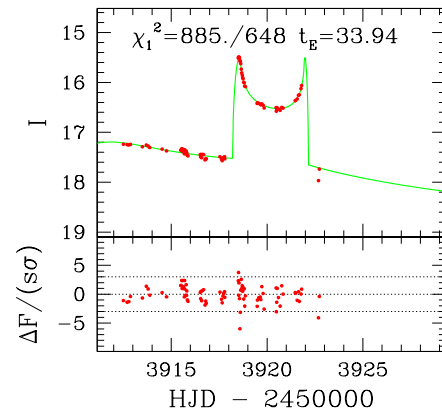
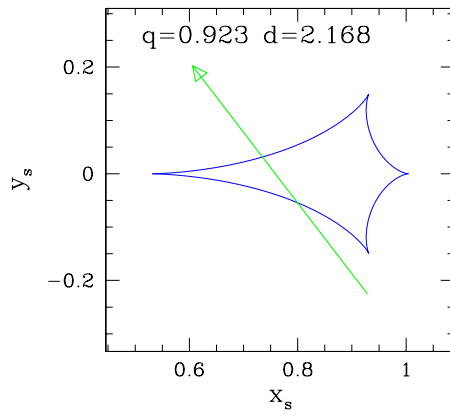
OGLE 2006-BLG-076**OGLE 2006-BLG-119****OGLE 2006-BLG-215**

OGLE 2006-BLG-277**OGLE 2006-BLG-284****OGLE 2006-BLG-304 (1st model)**

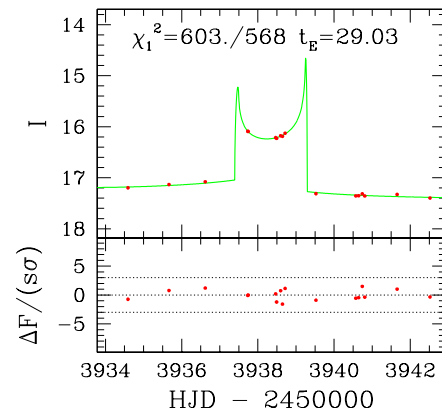
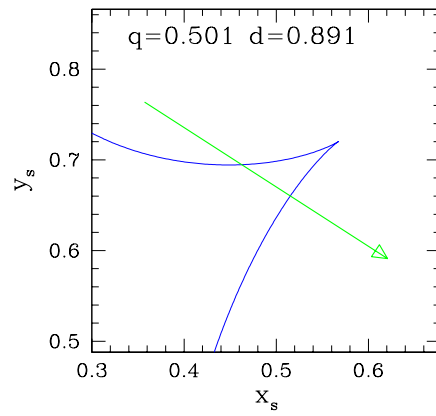
OGLE 2006-BLG-304 (2nd model)

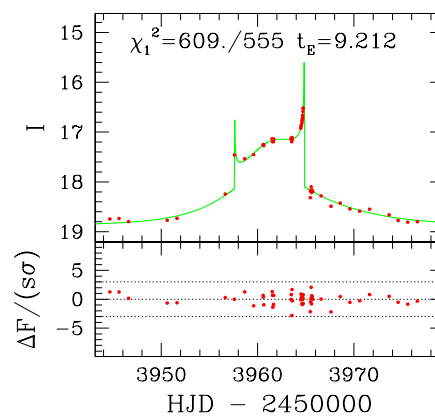
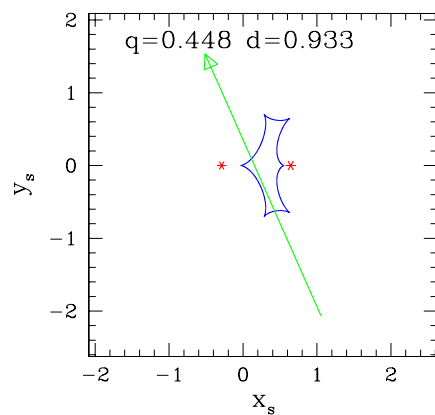
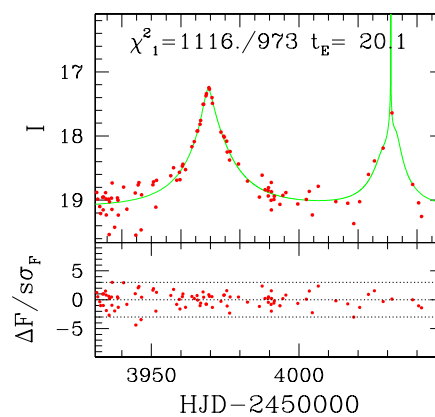
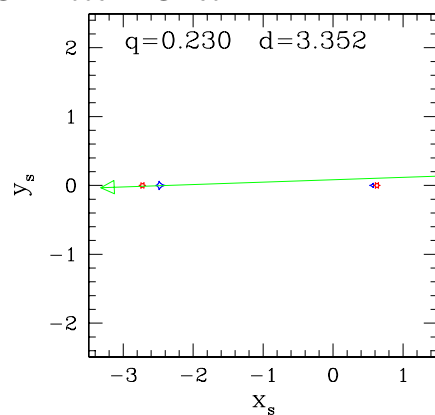
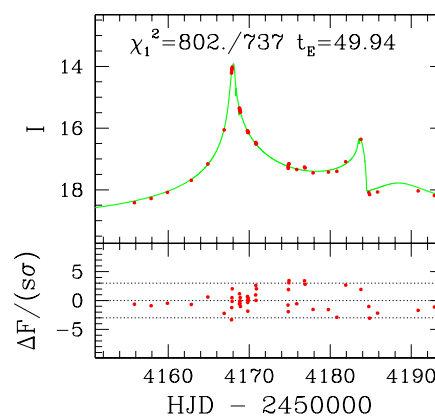
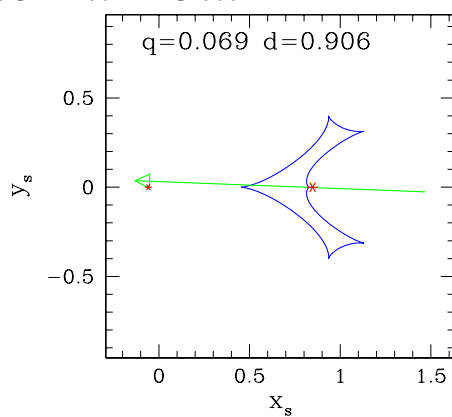


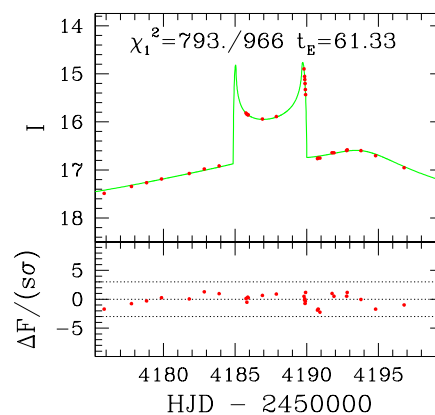
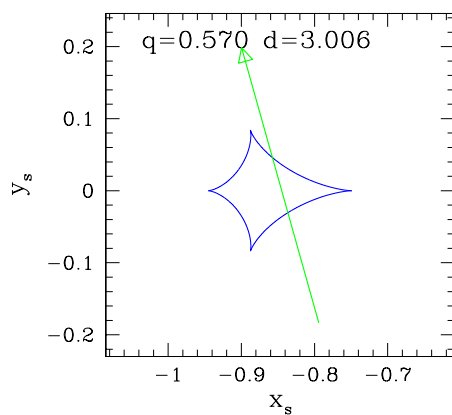
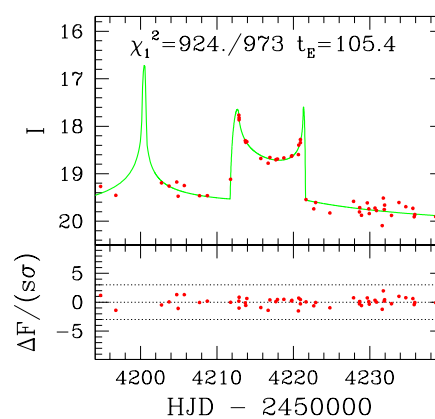
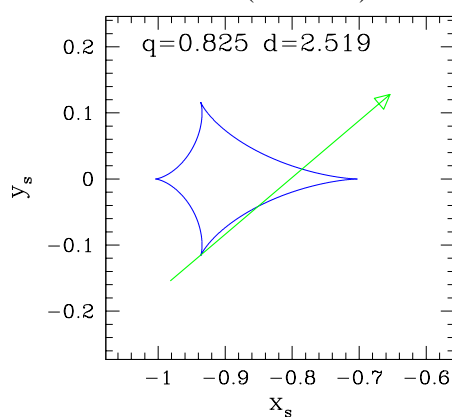
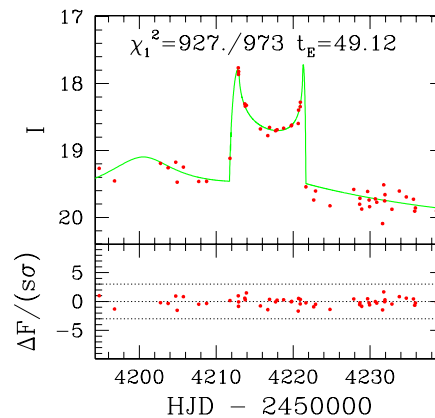
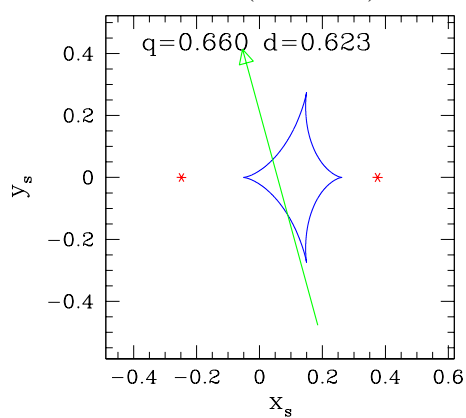
OGLE 2006-BLG-335

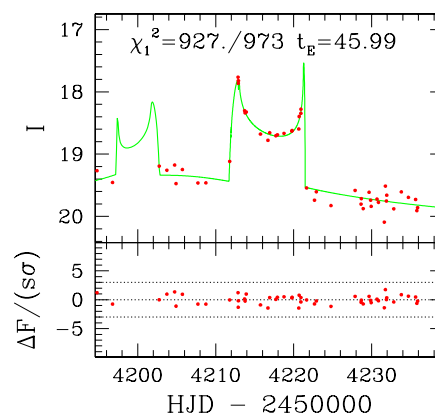
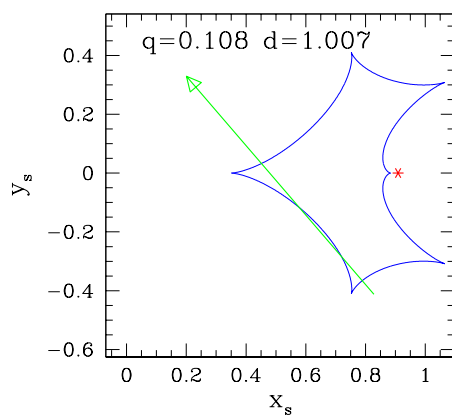
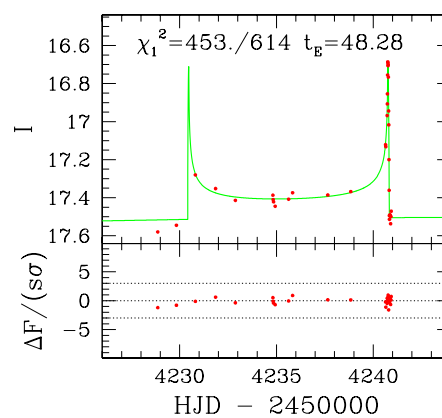
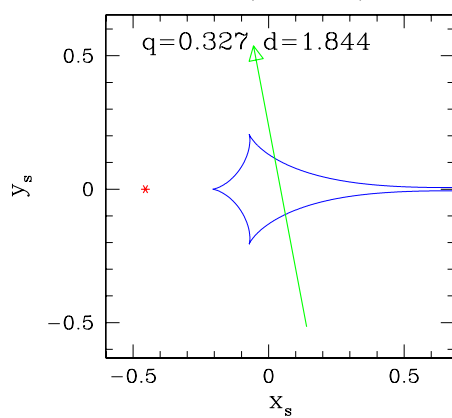
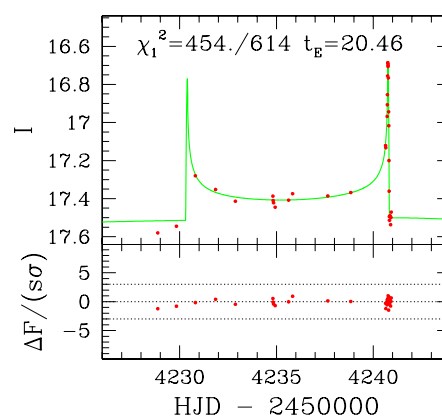
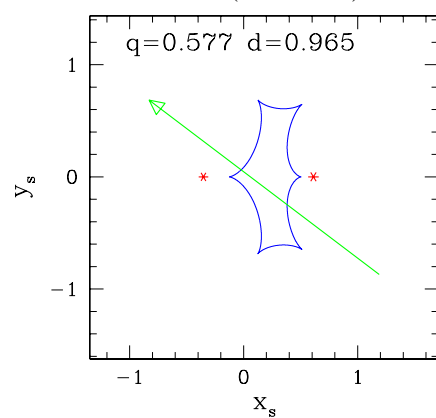


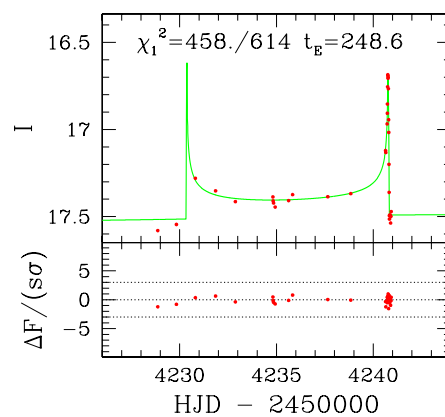
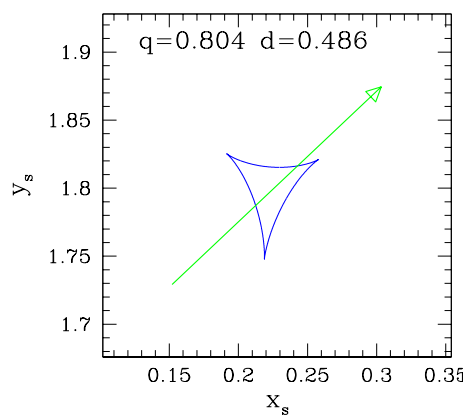
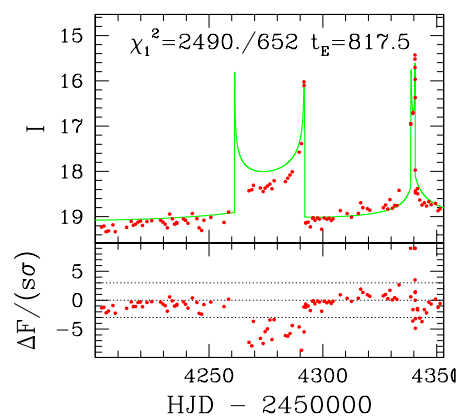
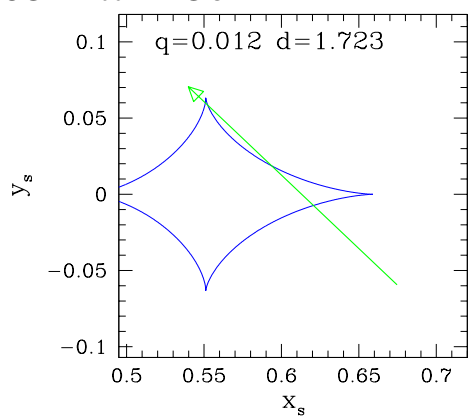
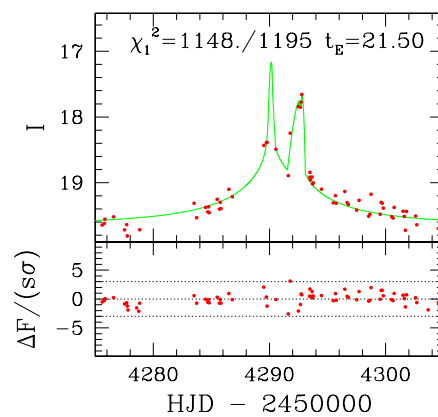
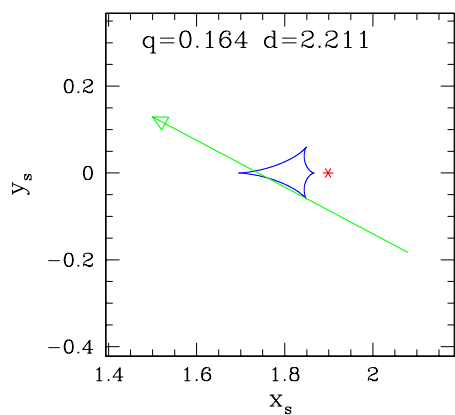
OGLE 2006-BLG-375

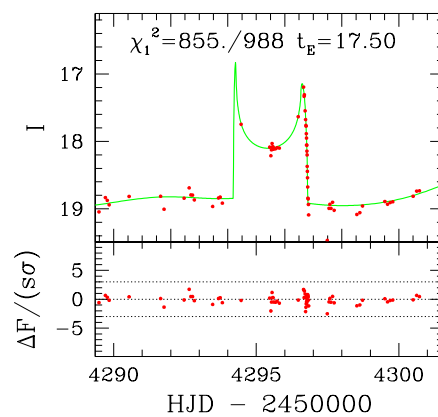
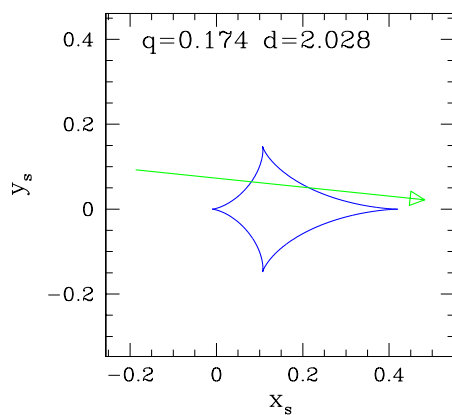
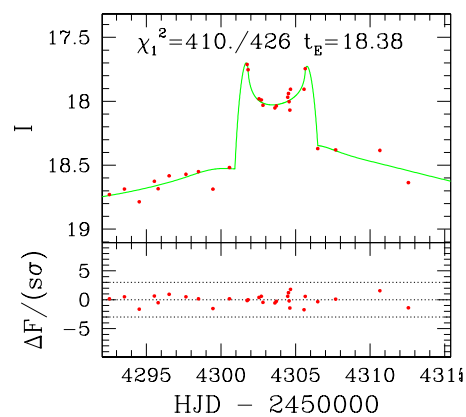
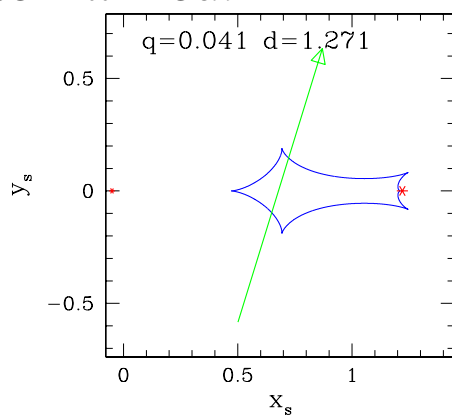
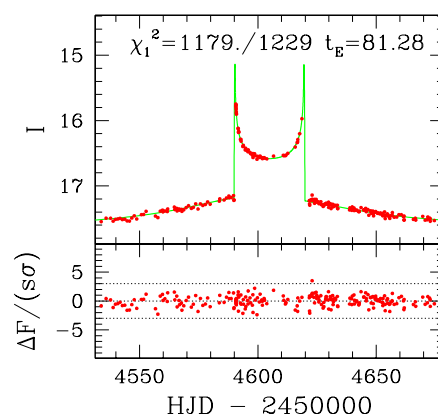
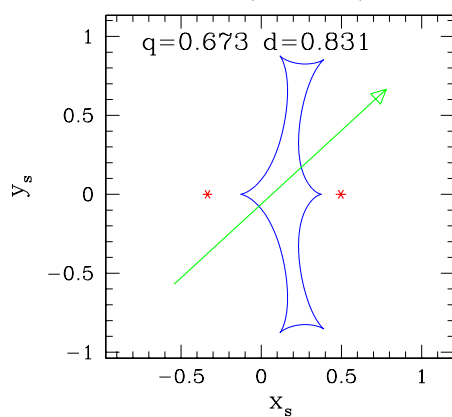


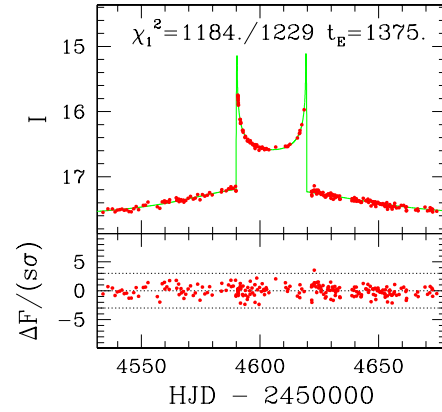
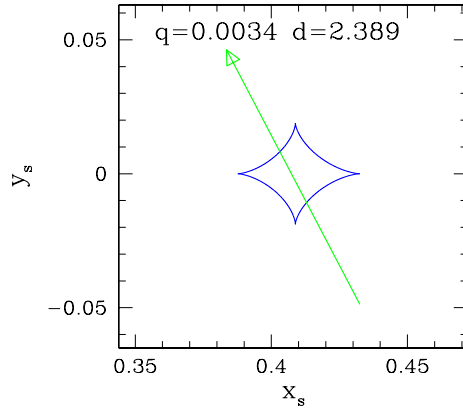
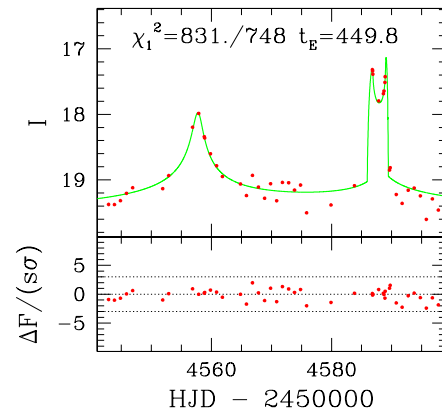
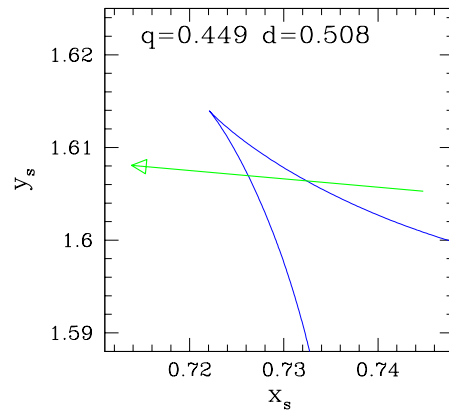
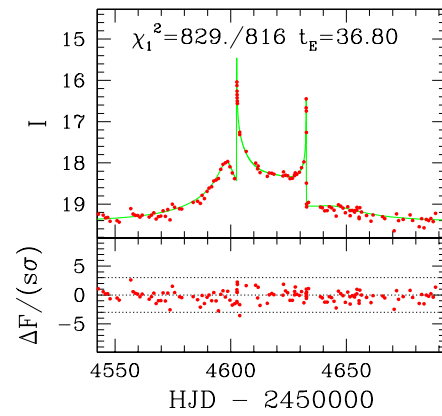
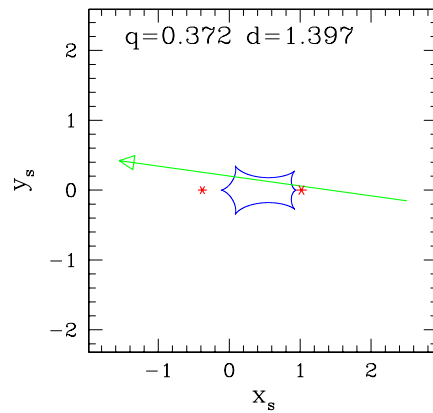
OGLE 2006-BLG-450**OGLE 2006-BLG-460****OGLE 2007-BLG-006**

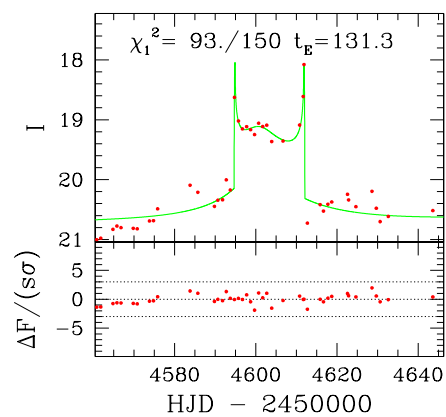
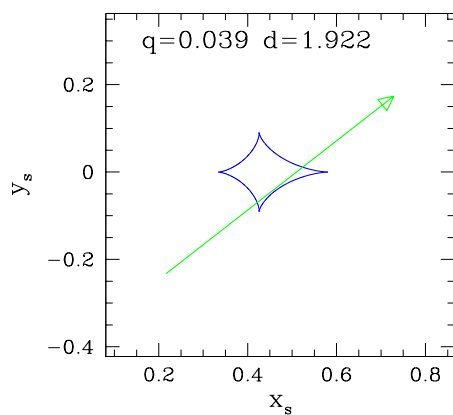
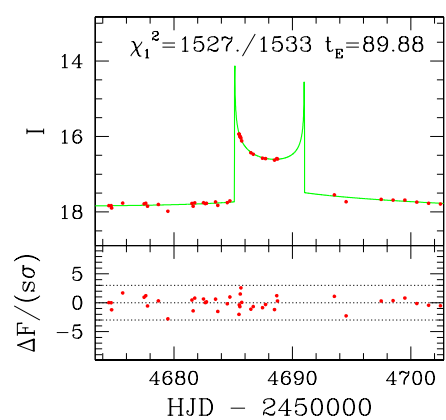
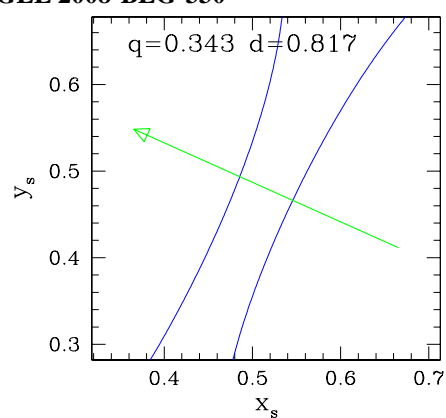
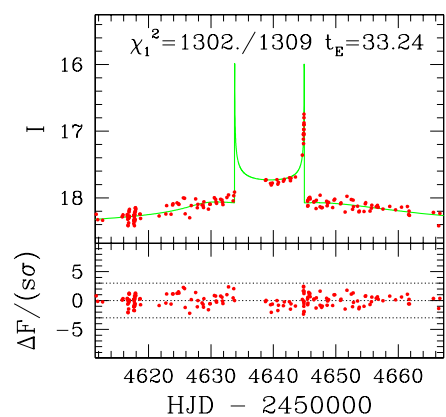
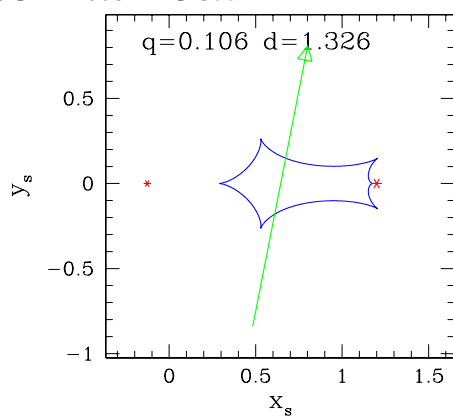
OGLE 2007-BLG-069**OGLE 2007-BLG-149 (1st model)****OGLE 2007-BLG-149 (2nd model)**

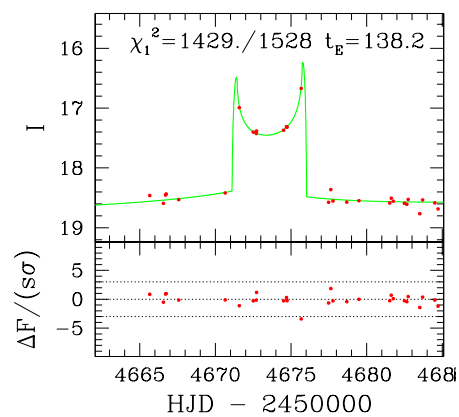
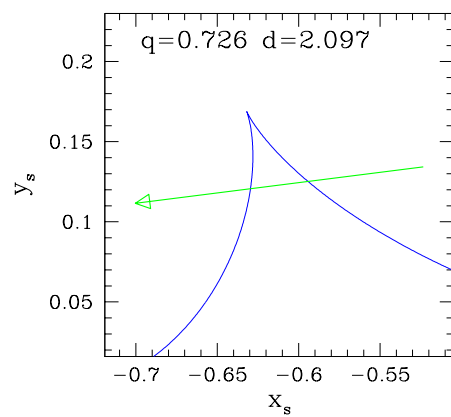
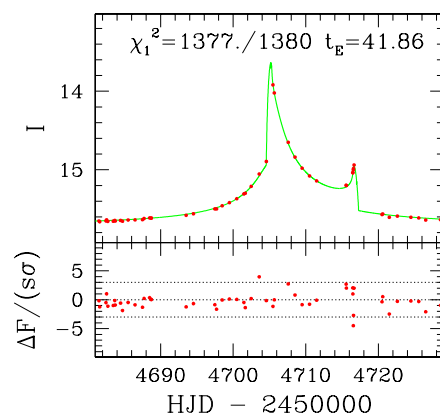
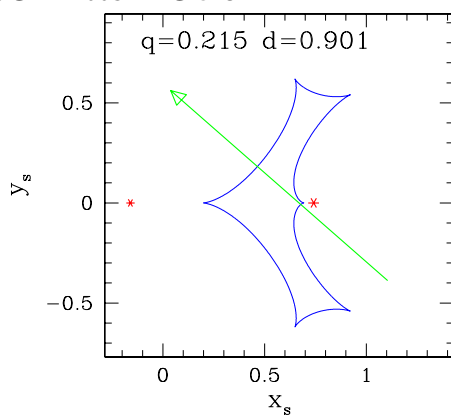
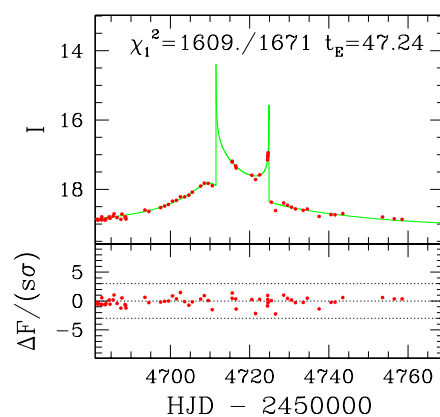
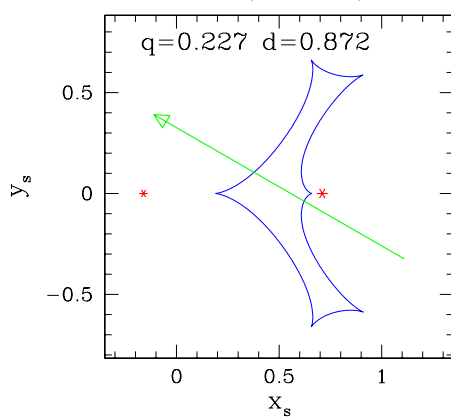
OGLE 2007-BLG-149 (3rd model)**OGLE 2007-BLG-237 (1st model)****OGLE 2007-BLG-237 (2nd model)**

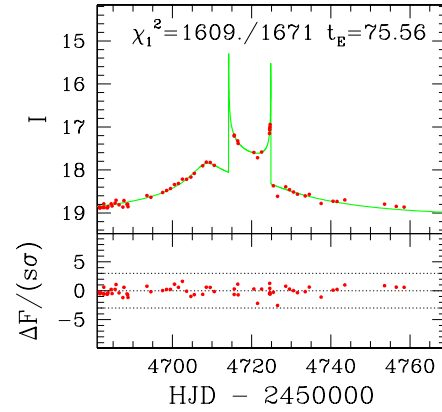
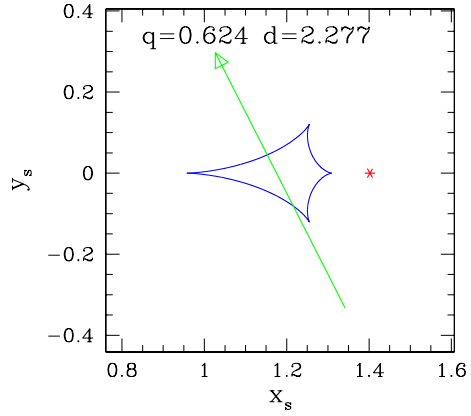
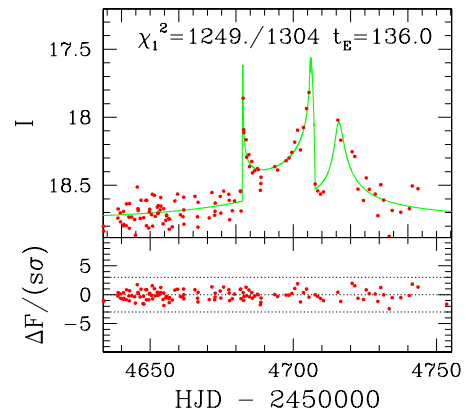
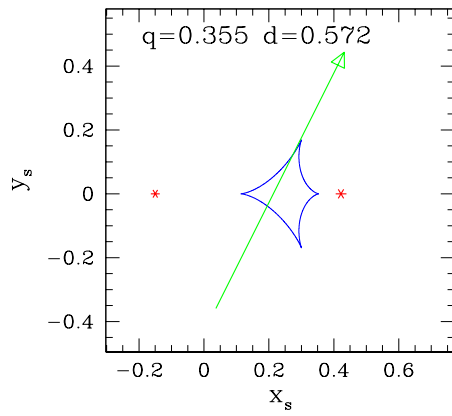
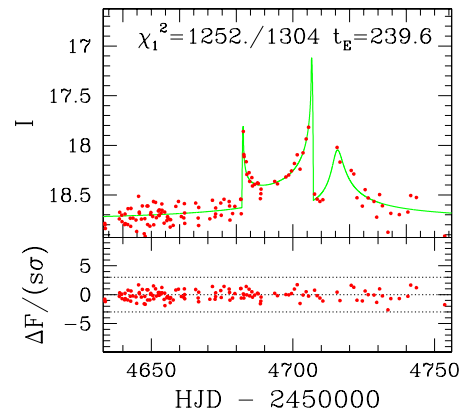
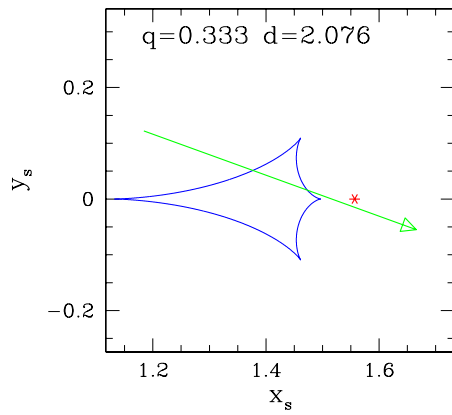
OGLE 2007-BLG-237 (3rd model)**OGLE 2007-BLG-327****OGLE 2007-BLG-363**

OGLE 2007-BLG-373**OGLE 2007-BLG-399****OGLE 2008-BLG-118 (1st model)**

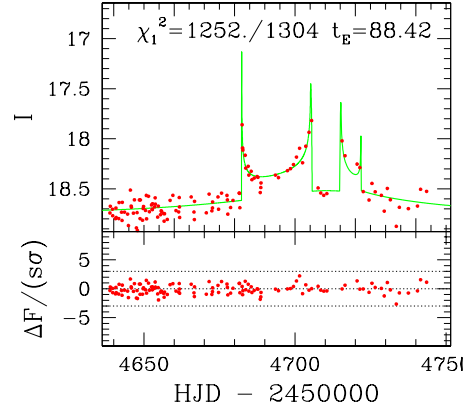
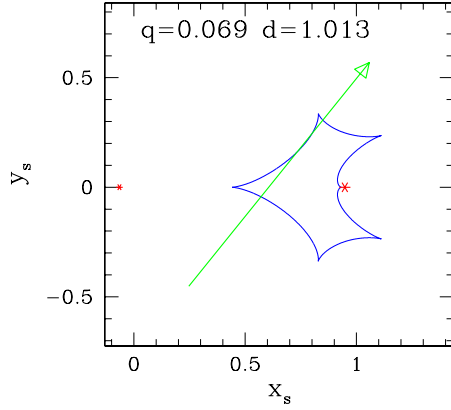
OGLE 2008-BLG-118 (2nd model)**OGLE 2008-BLG-125****OGLE 2008-BLG-243**

OGLE 2008-BLG-263**OGLE 2008-BLG-330****OGLE 2008-BLG-355**

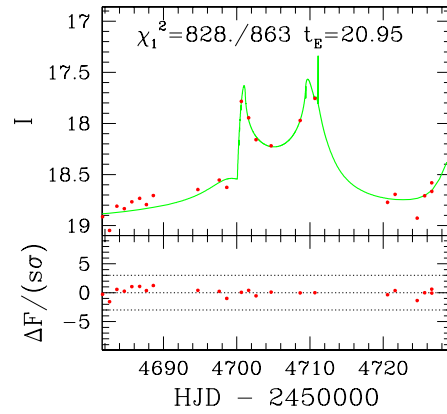
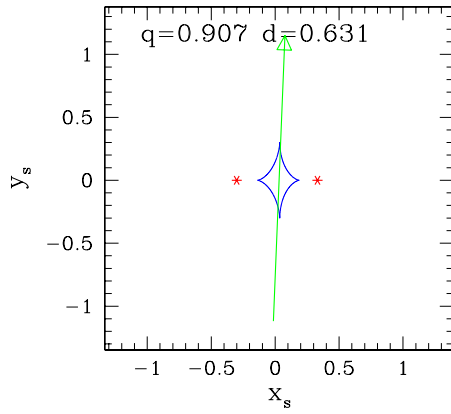
OGLE 2008-BLG-493**OGLE 2008-BLG-513****OGLE 2008-BLG-559 (1st model)**

OGLE 2008-BLG-559 (2nd model)**OGLE 2008-BLG-584 (1st model)****OGLE 2008-BLG-584 (2nd model)**

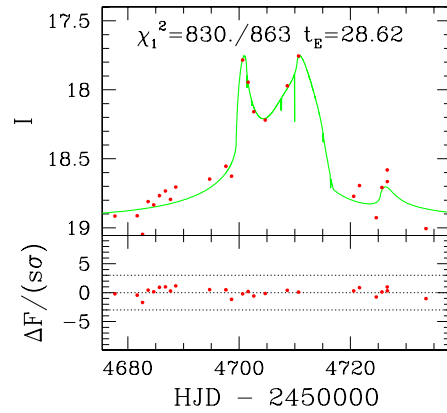
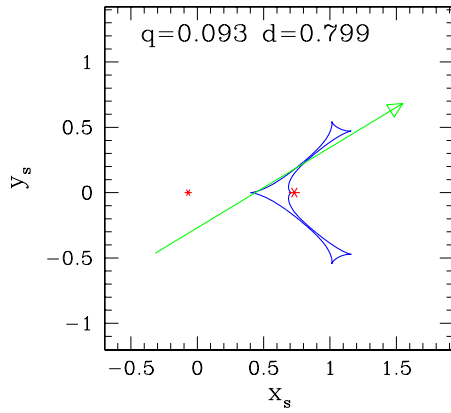
OGLE 2008-BLG-584 (3rd model)

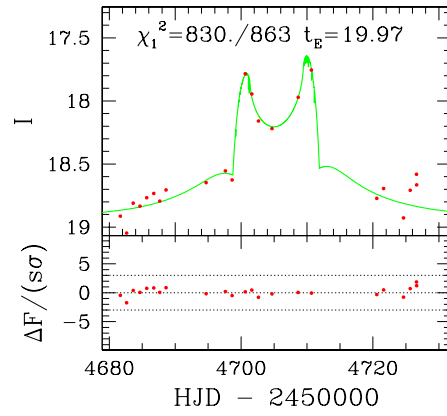
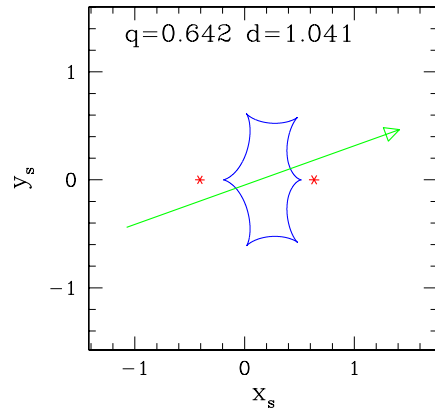


OGLE 2008-BLG-592 (1st model)



OGLE 2008-BLG-592 (2nd model)

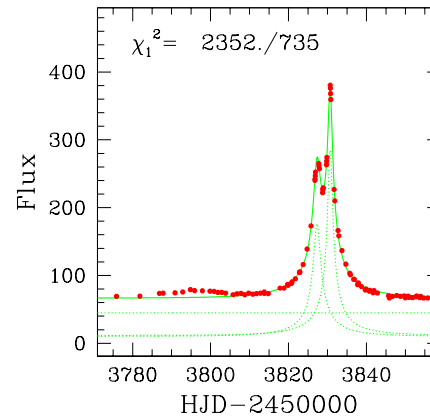
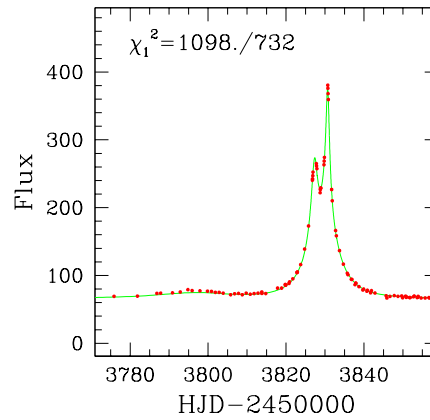


OGLE 2008-BLG-592 (3rd model)

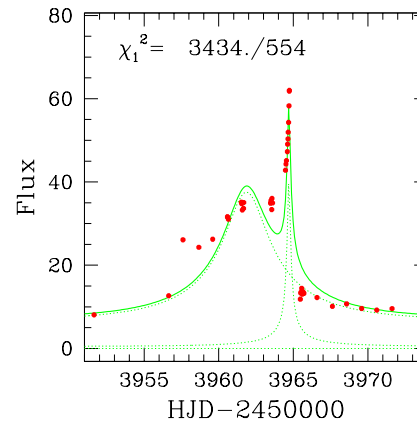
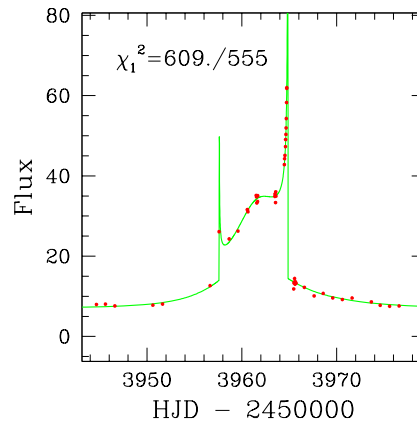
7.2 Comparison of binary lens and double source models

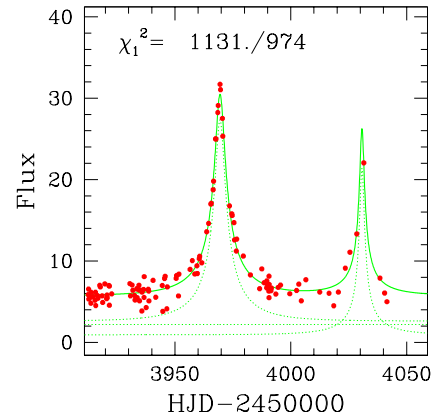
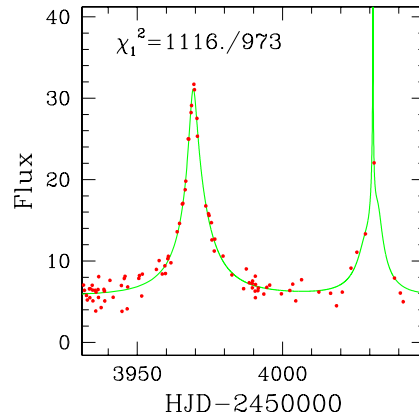
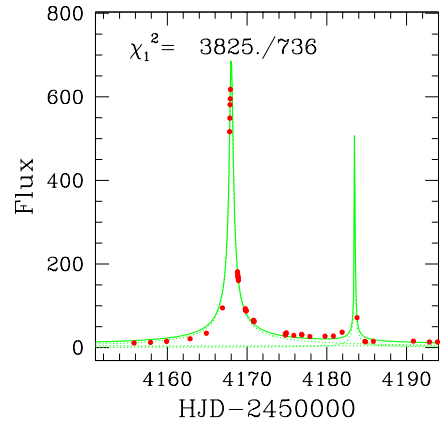
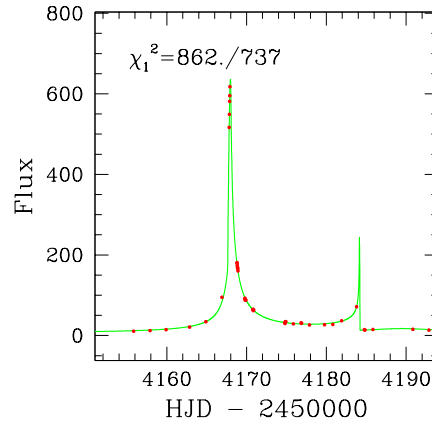
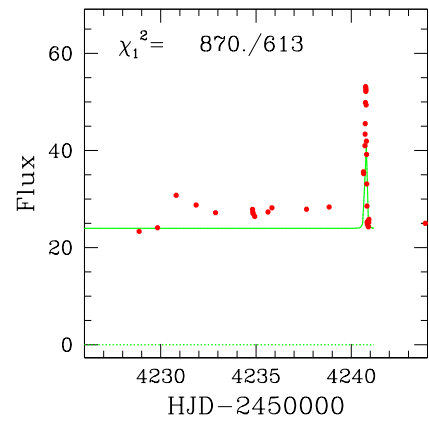
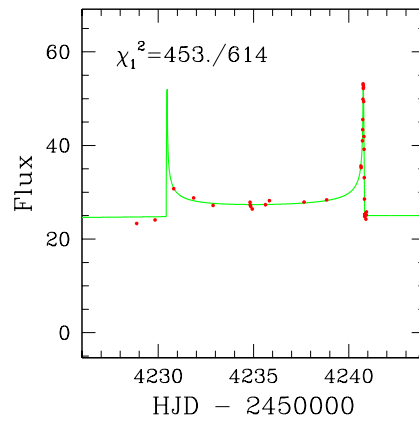
Below we show the binary lens (on the left) and double source (on the right) models of the light curves for some of the considered events. For all binary lens models we have also calculated double source models. We do not show events with evident jumps in the light curves, which can only be modeled as caustic crossings. We include, however, few cases with almost smooth observed light curves, despite the fact that their binary lens models are formally far better. The light curve in a double source model is a sum of the constant blended flux plus the two single lens light curves for the source components, each shown with dotted lines. In the plots we use observed fluxes (not magnitudes) since they are additive, which is important in double source modeling. In majority of cases the binary lens models give formally better fits as compared to the double source models presented. On the other hand double source models, always producing *simpler* light curves, look more natural in some cases.

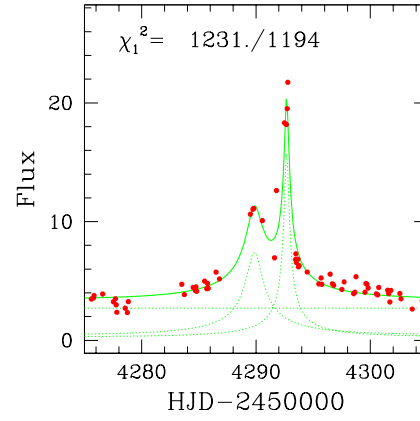
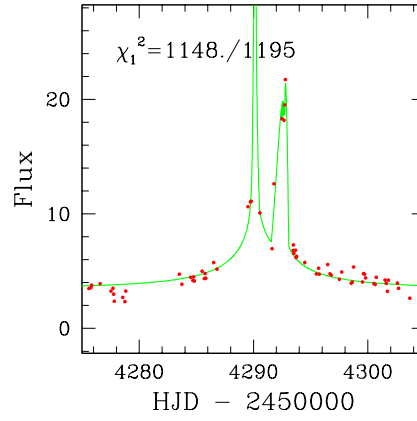
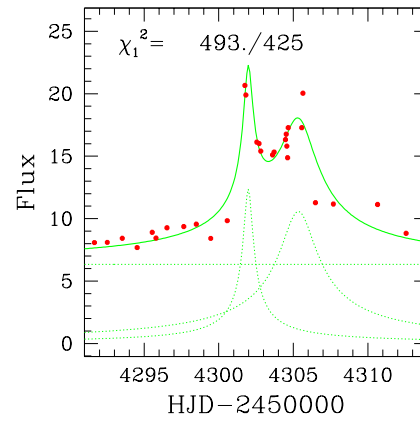
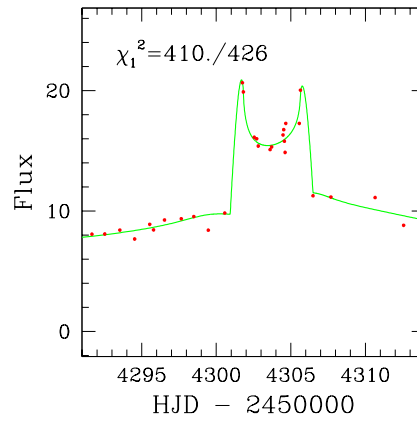
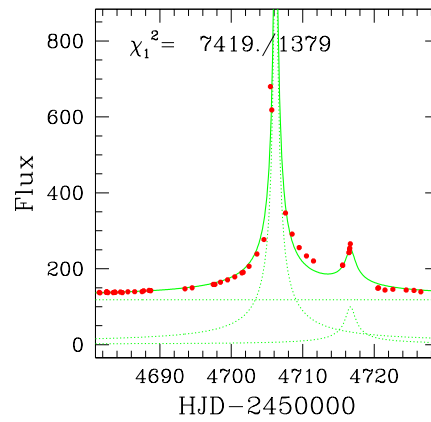
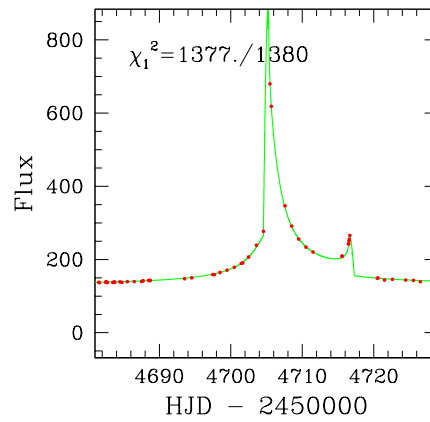
OGLE 2006-BLG-038

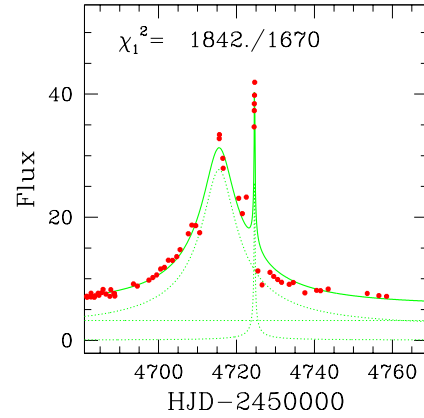
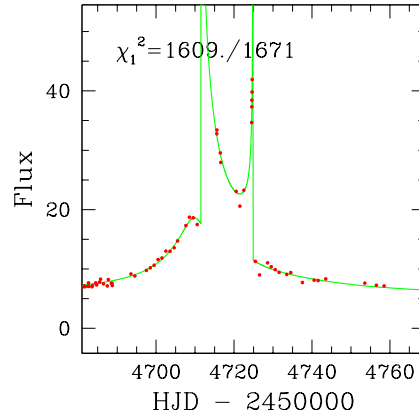
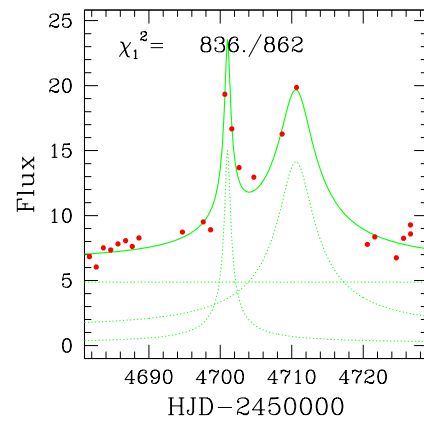
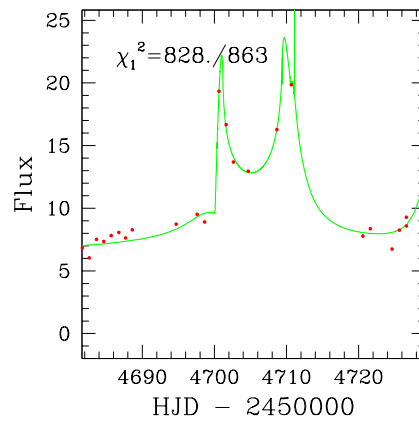
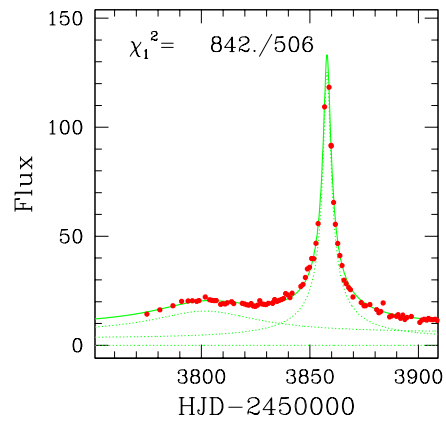
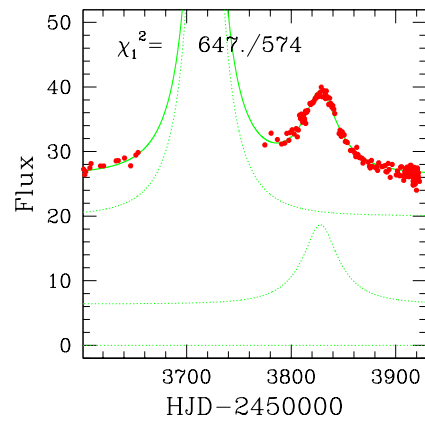


OGLE 2006-BLG-450

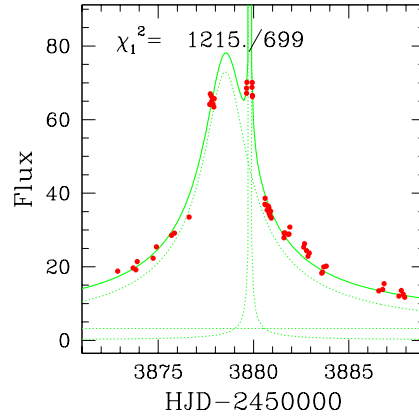


OGLE 2006-BLG-460**OGLE 2007-BLG-006****OGLE 2007-BLG-237**

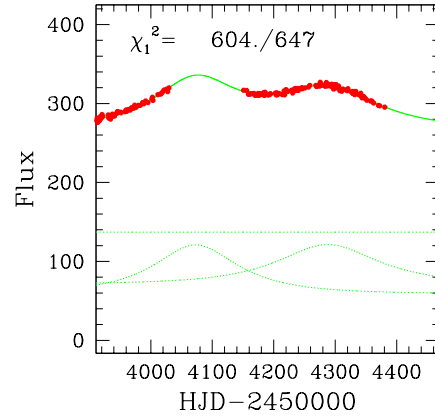
OGLE 2007-BLG-363**OGLE 2007-BLG-399****OGLE 2008-BLG-513**

OGLE 2008-BLG-559**OGLE 2008-BLG-592****7.3 Double source models****OGLE 2006-BLG-023****OGLE-2006-BLG-061**

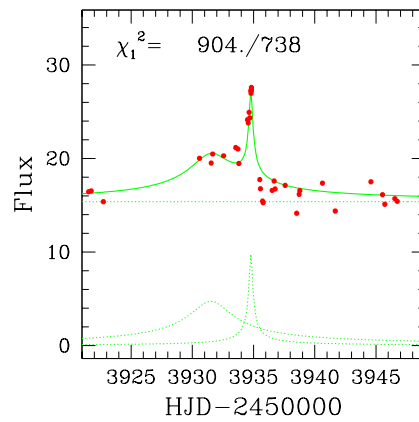
OGLE 2006-BLG-238



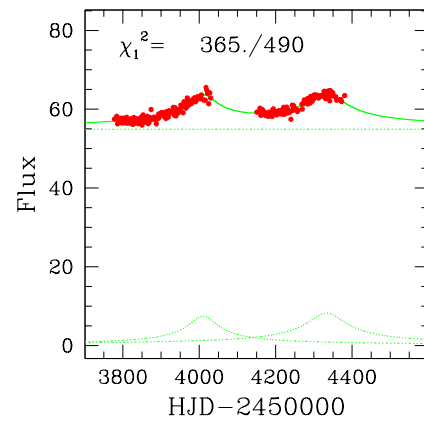
OGLE-2006-BLG-393



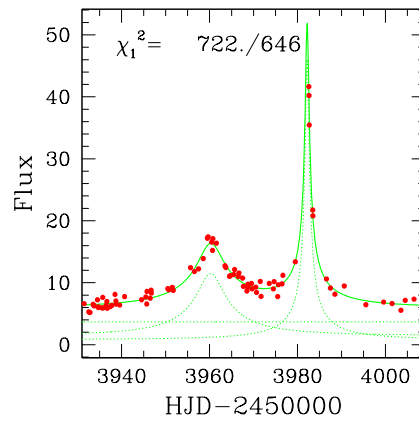
OGLE 2006-BLG-398



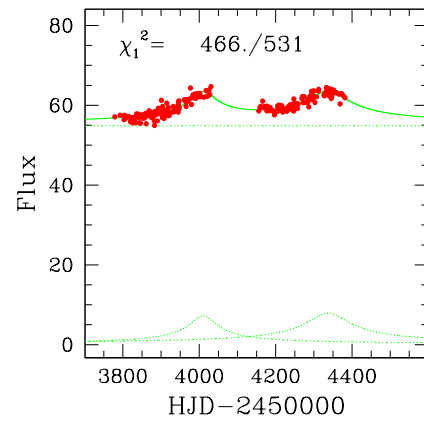
OGLE-2006-BLG-441



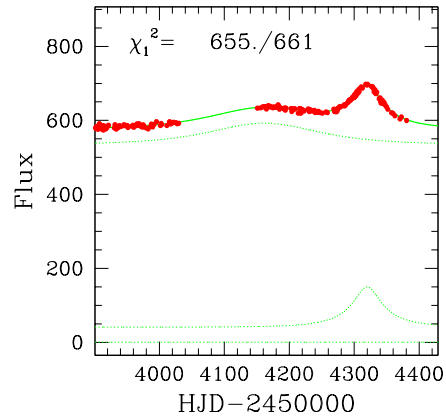
OGLE 2006-BLG-444



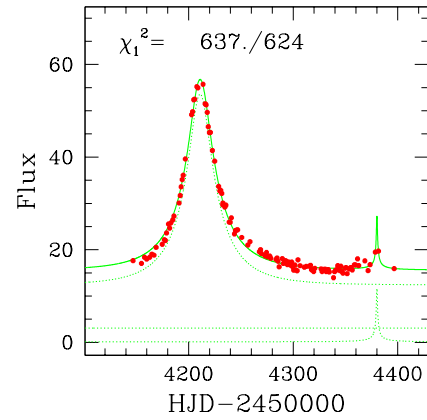
OGLE-2006-BLG-504



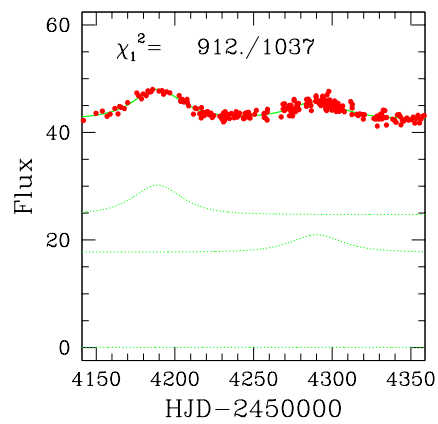
OGLE 2007-BLG-040



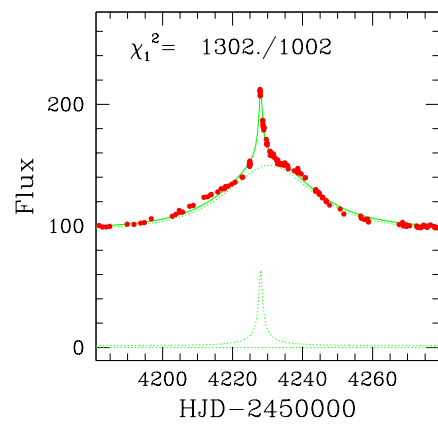
OGLE-2007-BLG-080



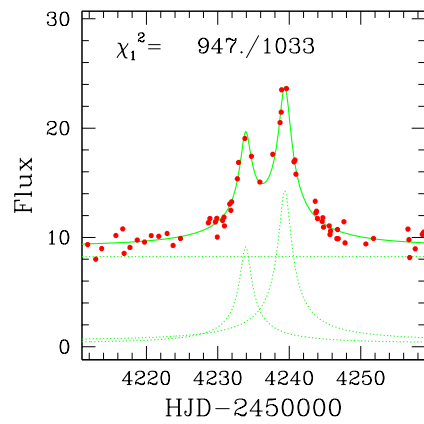
OGLE 2007-BLG-091



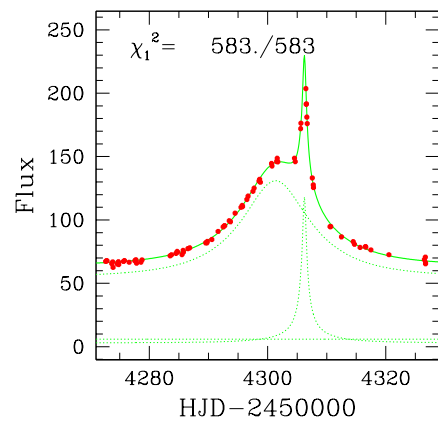
OGLE-2007-BLG-159



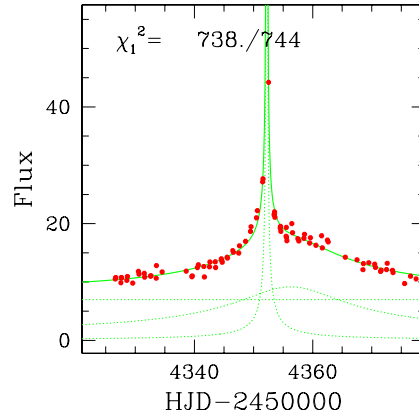
OGLE 2007-BLG-236



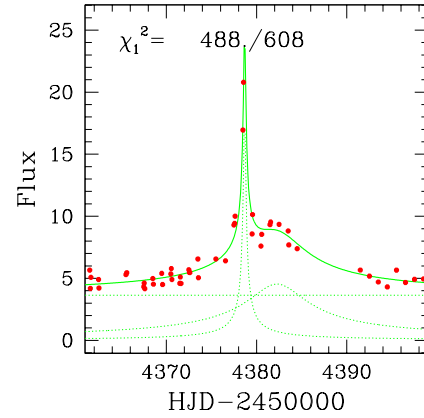
OGLE-2007-BLG-355



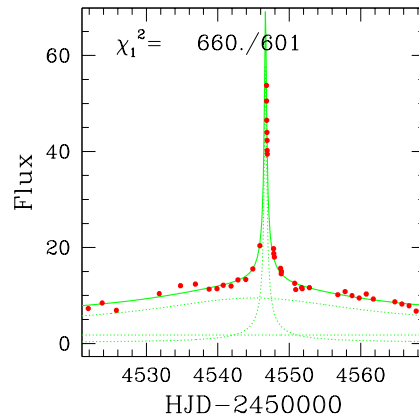
OGLE 2007-BLG-491



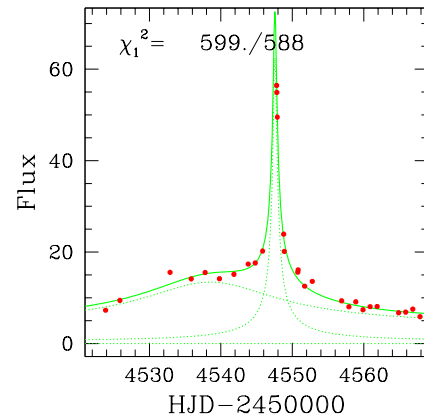
OGLE-2007-BLG-594



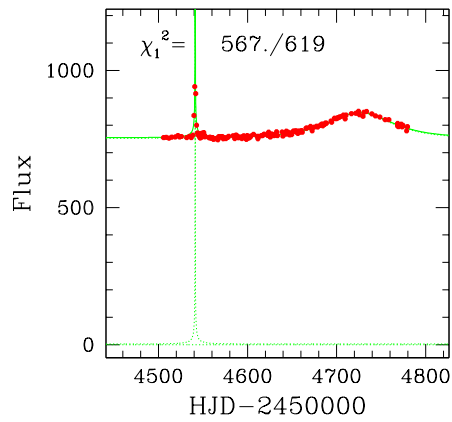
OGLE 2008-BLG-078



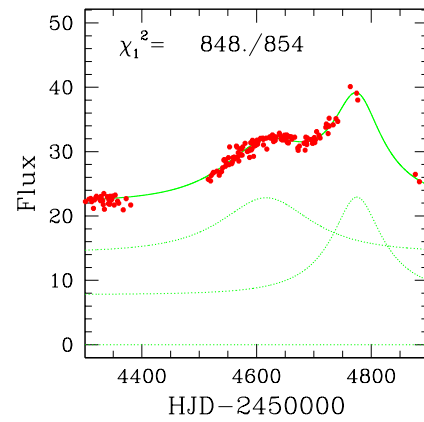
OGLE-2008-BLG-084



OGLE 2008-BLG-092



OGLE-2008-BLG-098



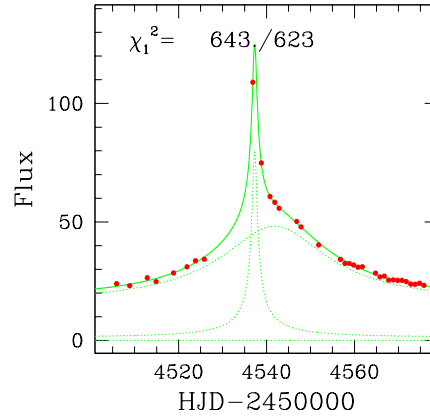
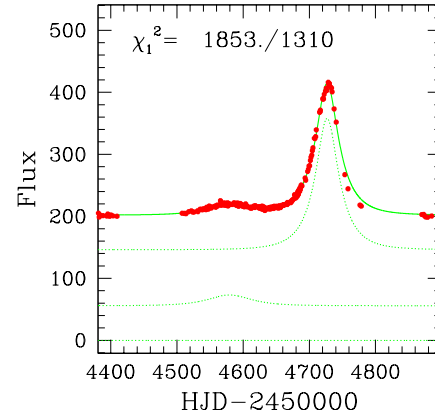
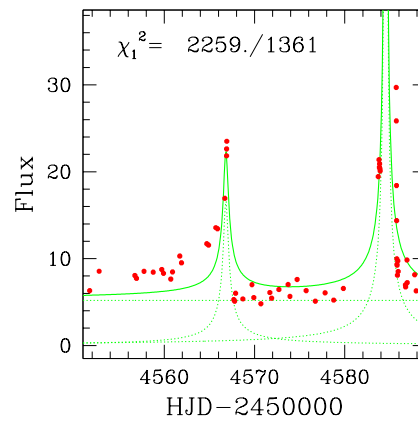
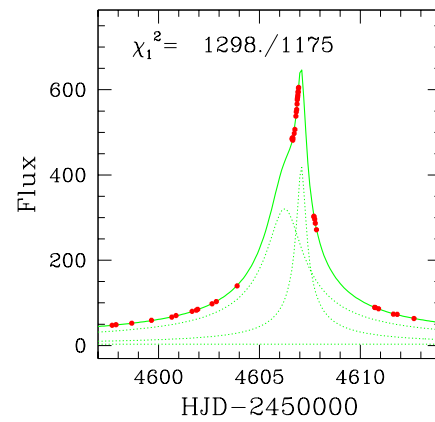
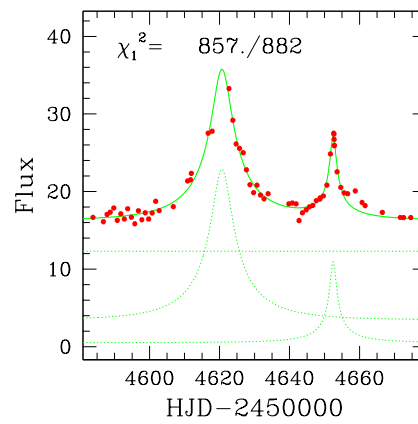
OGLE 2008-BLG-110**OGLE-2008-BLG-143****OGLE 2008-BLG-146****OGLE-2008-BLG-210****OGLE 2008-BLG-353**

Table 1
Binary lenses parameters, excluding known planetary cases

Event		χ_1^2/dof	s	q	d	β	b	t_0	t_E	f	r_s
06-028	b	919.6/770	1.89	0.195	1.086	1.73	-0.10	3799.6	41.6	0.39	
06-038	b	1097.8/732	1.79	0.618	3.116	153.67	0.64	3810.6	12.4	1.00	
06-076	b	1357.1/667	1.93	0.455	1.732	2.51	-0.02	3811.6	9.7	0.93	0.0104
06-119	u	1260.1/759	1.58	0.066	0.770	136.42	0.05	3842.0	63.1	0.19	
06-215	b	1131.4/804	4.08	0.959	0.991	152.12	-0.49	3855.2	28.9	0.69	0.0081
06-277	b	634.1/441	2.52	0.593	1.368	97.80	0.12	3941.3	38.1	0.99	0.0056
06-284	b	1437.2/601	1.81	0.242	0.820	23.56	0.10	3898.9	37.2	0.99	0.0008
06-304	b	1022.0/723	1.61	0.248	2.630	128.33	1.38	3844.9	49.8	0.53	0.0009
06-304	b	1023.7/723	1.61	0.308	0.628	54.93	0.06	3900.4	24.0	0.34	0.0010
06-335	b	884.6/648	1.82	0.923	2.168	127.01	-0.54	3934.4	33.9	0.98	0.0032
06-375	b	603.4/568	1.70	0.501	0.891	326.83	0.67	3944.4	29.0	0.93	
06-450	b	609.1/555	1.48	0.449	0.934	113.54	0.18	3963.2	9.2	0.88	
06-460	b	1115.7/973	1.47	0.230	3.352	181.36	-0.11	3981.2	20.1	0.67	
07-006	b	801.6/737	1.71	0.069	0.906	177.76	0.00	4169.9	49.9	0.67	
07-069	b	792.9/966	1.83	0.570	3.006	105.40	1.61	4159.7	61.3	0.55	0.0016
07-149	b	923.8/973	1.17	0.825	2.519	40.72	0.68	4302.4	105.4	0.25	
07-149	b	927.0/973	1.17	0.660	0.623	105.01	0.07	4217.6	49.1	0.26	
07-149	b	927.2/973	1.17	0.108	1.007	130.24	0.25	4209.5	46.0	0.55	
07-237	b	453.4/614	2.16	0.327	1.844	100.51	0.88	4227.3	48.3	0.05	0.0007
07-237	b	454.0/614	2.16	0.577	0.965	142.41	0.12	4235.5	20.5	0.04	0.0020
07-237	b	458.0/614	2.16	0.804	0.486	43.85	1.18	3893.9	248.6	0.07	0.0001
07-327	u	2489.8/652	1.87	0.012	1.723	136.06	0.74	3640.7	817.5	0.50	
07-363	d	1148.5/1195	1.32	0.164	2.211	151.68	-0.07	4295.6	21.5	0.13	
07-373	b	855.0/988	1.79	0.208	2.047	353.78	-0.08	4317.5	17.5	0.40	0.0023
07-399	b	409.7/426	1.24	0.041	1.271	73.09	0.47	4305.9	18.4	0.62	
08-118	b	1179.2/1229	1.53	0.673	0.831	43.05	0.07	4604.9	81.3	0.32	
08-118	b	1184.0/1229	1.53	0.003	2.389	117.28	1.75	3368.3	1374.7	0.33	
08-125	b	830.7/748	1.65	0.449	0.508	174.86	-1.65	4763.2	449.8	0.80	
08-243	b	828.6/816	1.30	0.372	1.397	171.93	-0.11	4611.0	36.8	0.71	0.0016
08-263	b	93.3/150	1.00	0.039	1.922	38.43	0.79	4740.2	131.3	0.59	
08-330	b	1526.9/1533	1.50	0.343	0.817	155.48	-0.48	4679.7	89.2	0.90	
08-355	b	1301.8/1309	1.88	0.106	1.326	79.11	0.42	4642.6	33.2	0.44	
08-493	b	1426.5/1528	1.71	0.726	2.097	187.30	-0.24	4554.7	129.0	0.24	
08-513	b	1377.4/1380	1.93	0.215	0.901	138.32	-0.06	4708.2	41.9	0.11	
08-559	b	1608.8/1671	1.29	0.227	0.872	149.65	0.00	4715.4	47.2	0.54	
08-559	b	1608.8/1671	1.29	0.624	2.277	116.60	-0.58	4742.9	75.6	0.31	
08-584	b	1249.3/1304	1.58	0.355	0.572	63.76	0.05	4691.6	136.0	0.03	
08-584	b	1251.6/1304	1.58	0.333	2.076	339.84	0.17	4610.2	239.6	0.03	
08-584	b	1251.9/1304	1.58	0.069	1.013	51.55	0.22	4702.5	88.4	0.10	
08-592	d	828.1/863	1.71	0.907	0.631	87.73	0.00	4705.1	21.0	0.10	
08-592	d	829.7/863	1.71	0.093	0.799	31.61	0.12	4706.2	28.6	0.15	
08-592	d	830.2/863	1.71	0.642	1.041	20.02	0.03	4706.4	20.0	0.31	

Note: The table contains all 2006–2008 seasons events, which have been modeled as binary lenses. The columns show: two last digits of the year and the EWS number, the event classification (“b” for binary lens, “d” for double source, “u” for unsatisfactory), the rescaled χ_1^2 / degree of freedom number, the scaling factor s ($\chi_1^2 = \chi_{\text{raw}}^2 / s^2$), the binary lens model parameters (see Section 3), and the blending parameter $f \equiv F_s / F_0$. For events with at least one resolved caustic crossing the size of the source r_s is given; otherwise it is omitted.

Table 2
Parameters of double source modeling

Event	χ^2/DOF	b_1	b_2	t_{01}	t_{02}	t_E	f_1	f_2
06-023	842./506	0.4066	0.0274	3801.59	3857.87	60.2	0.637	0.363
06-038	2352./735	0.0582	0.0409	3827.33	3830.68	15.4	0.154	0.175
06-061	647./574	0.0023	0.3595	3717.61	3827.98	45.5	0.758	0.242
06-238	1215./699	0.0458	0.0000	3878.53	3879.81	23.0	0.501	0.016
06-393	604./647	0.5400	0.6874	4073.06	4287.97	135.5	0.221	0.267
06-398	904./738	0.0047	0.0004	3931.52	3934.78	356.7	0.001	0.000
06-441	365./490	0.0385	0.0508	4009.75	4333.22	962.2	0.005	0.008
06-444	722./646	0.1325	0.0186	3960.27	3982.20	23.9	0.250	0.142
06-450	3434./554	0.1767	0.0119	3961.86	3964.70	8.4	0.931	0.069
06-460	1131./974	0.0958	0.0435	3969.47	4030.73	23.6	0.455	0.162
06-504	466./531	0.0415	0.0647	4010.02	4337.93	845.8	0.005	0.009
07-006	3825./736	0.0013	0.0000	4168.02	4183.50	161.5	0.173	0.019
07-040	655./661	1.6218	0.2823	4161.42	4319.90	76.4	0.928	0.071
07-080	637./624	0.2360	0.0110	4211.02	4380.11	49.7	0.795	0.008
07-091	912./1037	1.2175	1.3241	4188.87	4290.17	17.2	0.582	0.417
07-159	1302./1002	0.0247	0.7771	4228.01	4230.65	19.0	0.016	0.984
07-236	947./1033	0.0383	0.0429	4233.90	4239.38	20.1	0.038	0.066
07-237	870./613	0.0059	0.4840	4208.92	4240.76	0.1	0.000	1.000
07-355	583./583	0.4516	0.0257	4301.36	4306.21	13.1	0.861	0.047
07-363	1231./1194	0.0178	0.0592	4289.86	4292.68	11.9	0.082	0.127
07-399	493./425	0.0018	0.0069	4301.98	4305.34	173.9	0.003	0.011
07-491	738./744	0.0000	0.1769	4352.25	4356.28	51.8	0.019	0.183
07-594	488./608	0.0023	0.0520	4378.67	4382.26	61.8	0.011	0.060
08-078	660./601	0.4376	0.0039	4545.08	4546.68	33.6	0.659	0.040
08-084	599./588	0.3480	0.0101	4538.52	4547.57	27.2	0.877	0.123
08-092	567./619	0.0001	1.5498	4541.25	4726.12	34.0	0.003	0.997
08-098	848./854	0.7560	0.3552	4616.70	4774.99	120.7	0.648	0.352
08-110	643./623	0.0175	0.3668	4537.30	4541.81	32.2	0.076	0.924
08-143	1853./1310	1.0437	0.4371	4579.51	4726.86	40.3	0.276	0.724
08-146	2259./1361	0.0000	0.0000	4566.83	4584.53	30628.0	0.000	0.000
08-210	1298./1175	0.0433	0.0113	4606.25	4607.07	19.5	0.639	0.219
08-353	857./882	0.1527	0.0478	4620.69	4652.47	20.2	0.213	0.032
08-513	7419./1379	0.0087	0.0184	4706.21	4716.68	36.4	0.072	0.014
08-559	1842./1670	0.0894	0.0024	4715.51	4724.62	45.1	0.429	0.011
08-592	836./862	0.0178	0.1071	4701.01	4710.59	22.2	0.040	0.226

Note: The table contains two last digits of the year and the EWS number, the rescaled χ^2 value and the DOF number, the impact parameters b_1 and b_2 for the two source components, times of the closest approaches t_{01} and t_{02} , the Einstein time t_E , and the blending parameters $f_1 = F_{s1}/(F_{s1} + F_{s2} + F_b)$ and $f_2 = F_{s2}/(F_{s1} + F_{s2} + F_b)$.

